
Article:
Wielstra, B. orcid.org/0000-0002-7112-5965, McCartney-Melstad, E., Arntzen, J.W. et al. (2 more authors) (2019) Phylogenomics of the adaptive radiation of Triturus newts supports gradual ecological niche expansion towards an incrementally aquatic lifestyle. Molecular Phylogenetics and Evolution, 133. pp. 120-127. ISSN 1055-7903

https://doi.org/10.1016/j.ympev.2018.12.032

Running head: **Phylogenomics of *Triturus* newts**

Phylogenomics of the adaptive radiation of *Triturus* newts supports gradual ecological niche expansion towards an incrementally aquatic lifestyle

B. Wielstra[a,b,c,d,1,*], E. McCartney-Melstad[a,e,1], J.W. Arntzen[c], R.K. Butlin[b,f], H.B. Shaffer[a,e]

[a] *Department of Ecology and Evolutionary Biology, University of California, Los Angeles, CA 90095, USA.*

[b] *Department of Animal and Plant Sciences, University of Sheffield, S10 2TN Sheffield, UK.*

[c] *Naturalis Biodiversity Center, 2300 RA Leiden, The Netherlands.*

[d] *Institute of Biology Leiden, Leiden University, 2300 RA, Leiden, The Netherlands.*

[e] *La Kretz Center for California Conservation Science, Institute of the Environment and Sustainability, University of California, Los Angeles, CA 90095, USA.*

[f] *Department of Marine Sciences, University of Gothenburg, Gothenburg 405 30, Sweden.*

[1] *These authors contributed equally to this work.*

* *Corresponding author; e-mail: ben.wielstra@naturalis.nl*

Abstract

Newts of the genus *Triturus* (marbled and crested newts) exhibit substantial variation in the number of trunk vertebrae (NTV) and a higher NTV corresponds to a longer annual aquatic period. Because the *Triturus* phylogeny has thwarted resolution to date, the evolutionary history of NTV, annual aquatic period, and their potential coevolution has remained unclear. To resolve the phylogeny of *Triturus*, we generated a c. 6,000 transcriptome-derived marker data set using a custom target enrichment probe set, and conducted phylogenetic analyses using: 1) data concatenation with RAxML, 2) gene-tree summary with ASTRAL, and 3) species-tree estimation with SNAPP. All analyses produce the same, highly supported topology, despite cladogenesis having occurred over a short timeframe, resulting in short internal branch lengths. Our new phylogenetic hypothesis is consistent with the minimal number of inferred changes in NTV count necessary to explain the diversity in NTV observed today. Although a causal relationship between NTV, body form, and aquatic ecology has yet to be experimentally established, our phylogeny indicates that these features have evolved together, and suggest that they may underlie the adaptive radiation that characterizes *Triturus*.

Keywords: morphology; phylogeny; sequence capture; systematics; target enrichment; transcriptome

1. Introduction

Accurately retracing the evolution of phenotypic diversity in adaptive radiations requires well-established phylogenies. However, inferring the true branching order in adaptive radiations is hampered by the short time frame over which they typically unfold, which provides little opportunity between splitting events for phylogenetically informative substitutions to become established (resulting in low phylogenetic resolution; Philippe et al., 2011; Whitfield and Lockhart, 2007) and fixed (resulting in incomplete lineage sorting and discordance among gene-trees; Degnan and Rosenberg, 2006; Pamilo and Nei, 1988; Pollard et al., 2006). Resolving the phylogeny of rapidly multiplying lineages becomes even more complicated the further back in time the radiation occurred, because the accumulation of parallel substitutions along terminal branches can lead to long-branch attraction (Felsenstein, 1978; Swofford et al., 2001). A final impediment is reticulation between closely related (and not necessarily sister-) species through past or ongoing hybridization, resulting in additional gene-tree/species-tree discordance (Kutschera et al., 2014; Leaché et al., 2014; Mallet et al., 2016).

Phylogenomics, involving the consultation of a large number of markers spread throughout the genome, has proven successful in resolving both recent (e.g. Giarla and Esselstyn, 2015; Leaché et al., 2016; Léveillé-Bourret et al., 2018; Meiklejohn et al., 2016; Nater et al., 2015; Scott et al., 2018; Shi and Yang, 2018) and more ancient (e.g. Crawford et al., 2012; Irisarri and Meyer, 2016; Jarvis et al., 2014; McCormack et al., 2012; Song et al., 2012) evolutionary radiations. The appeal of greatly increasing the amount of data available for any given phylogenetic problem is that it often (but not always; see Philippe et al., 2011) provides informative characters to resolve short branches in the tree of life. Advances in laboratory and sequencing techniques, bioinformatics, and tree-building methods all facilitate phylogenetic reconstruction based on thousands of homologous loci for a large number of individuals, and promise to help provide the phylogenetic trees necessary to interpret the

evolution of eco-morphological characters involved in adaptive radiations (Alföldi et al., 2011; Stroud and Losos, 2016). In this study, we conduct a phylogenomic analysis of an adaptive radiation that moderately-sized multilocus nuclear DNA datasets (Arntzen et al., 2007; Espregueira Themudo et al., 2009; Wielstra et al., 2014) have consistently failed to resolve: the Eurasian newt genus *Triturus* (Amphibia: Urodela: Salamandridae), commonly known as the marbled and crested newts.

One of the most intriguing features of *Triturus* evolution is the correlation between certain aspects of their ecology and the number of trunk vertebrae (NTV; Fig. 1). Species characterized by a higher modal NTV (which translates into a more elongate body build with proportionally shorter limbs) are associated with a more aquatic lifestyle. Empirically, the number of months a *Triturus* species spends in the water (defined at the population level as the peak date of emigration, leaving a breeding pond, minus the peak in immigration, entering it) roughly equals NTV minus 10 (Arntzen, 2003; Arntzen and Wallis, 1999; Slijepčević et al., 2015). The intrageneric variation in NTV shown by *Triturus*, ranging from 12 to 17, is unparalleled in the family Salamandridae (Arntzen et al., 2015; Lanza et al., 2010) and a causal relationship between NTV expansion and an increasingly aquatic lifestyle has been presumed, but never adequately placed into a phylogenetic comparative analysis (Arntzen, 2003; Arntzen et al., 2015; Arntzen and Wallis, 1999; Govedarica et al., 2017; Slijepčević et al., 2015; Urošević et al., 2016; Vukov et al., 2011; Wielstra and Arntzen, 2011). A well-established *Triturus* species-tree is required to accurately retrace NTV evolution and assess the concordance between aquatic lifestyle and NTV across the genus.

Our goal is to obtain a genome-enabled phylogeny for *Triturus* and use it to reconstruct the eco-morphological evolution of NTV and aquatic/terrestrial ecology across the genus. As the large size of salamander genomes hampers whole-genome sequencing (but see Elewa et al., 2017; Nowoshilow et al., 2018; Smith et al., 2018), we employ a genome-reduction approach

in which we capture and sequence a set of transcriptome-derived markers using target enrichment, an efficient technique that affords extremely high resolution at multiple taxonomic levels (Abdelkrim et al., 2018; Bi et al., 2012; Bragg et al., 2016; Gnirke et al., 2009; McCartney-Melstad et al., 2016; McCartney-Melstad et al., 2018). Using data concatenation (with RAxML), gene-tree summarization (with ASTRAL) and species-tree estimation (with SNAPP), we fully resolve the *Triturus* phylogeny and place the extreme body shape and ecological variation observed in this adaptive radiation into an evolutionary context.

2. Materials and Methods

2.1 Target capture array design

Nine *Triturus* newts (seven crested and two marbled newt species) and one banded newt (*Ommatotriton*) were subjected to transcriptome sequencing. Transcriptome assemblies for each species were generated using Trinity v2.2.0 (Grabherr et al., 2011), clustered at 90% using usearch v9.1.13 (Edgar, 2010), and subjected to reciprocal best blast hit analysis (Bork et al., 1998; Camacho et al., 2009; Tatusov et al., 1997) to produce a set of *T. dobrogicus* transcripts (the species with the highest quality transcriptome assembly) that had putative orthologues present in the nine other transcriptome assemblies. These transcripts were then annotated using blastx to *Xenopus tropicalis* proteins, retaining one annotated transcript per protein. We attempted to discern splice sites in the transcripts, as probes spanning splice boundaries may perform poorly (Neves et al., 2013), by mapping transcripts iteratively to the genomes of *Chrysemys picta* (Shaffer et al., 2013), *X. tropicalis* (Hellsten et al., 2010), *Nanorana parkerii* (Sun et al., 2015) and *Rana catesbeiana* (Hammond et al., 2017). A single exon ≥ 200bp and ≤ 450bp was retained for each transcript target. To increase the ability of the target set to capture markers across all *Triturus* species, orthologous sequences from multiple species were

included for targets with > 5% sequence divergence from *T. dobrogicus* (Bi et al., 2012). We generated a target set of 7,102 genomic regions for a total target length of approximately 2.3 million bp. A total of 39,143 unique RNA probes were synthesized as a MyBaits-II kit for this target set at approximately 2.6X tiling density by Arbor Biosciences (Ann Arbor, MI, Ref# 170210-32). A detailed outline of the target capture array design process is presented in Supplementary Text S1.

2.2 Sampling scheme

We sampled 23 individual *Triturus* newts (Fig. 2; Supplementary Table S1) for which tissues were available from previous studies (Wielstra et al., 2017a; Wielstra et al., 2017b; Wielstra et al., 2013). Because the sister-group relationship between the two marbled and seven crested newts is well established (Fig. 1), while the relationships among the crested newt species have defied resolution, we sampled the crested newt species more densely, including three individuals per species to include intraspecific differentiation and to avoid misleading phylogenies resulting from single exemplar sampling (Spinks et al., 2013). Because *Triturus* species show introgressive hybridization at contact zones (Arntzen et al., 2014), we aimed to reduce the impact of interspecific gene flow by only including individuals that originate away from hybrid zones and have previously been interpreted as unaffected by interspecific genetic admixture (Wielstra et al., 2017a; Wielstra et al., 2017b). The reality of phylogenetic distortion by interspecific gene flow was underscored in a test for the phylogenetic utility of the transcripts used for marker design which included a genetically admixed individual (details in Supplementary Text S1).

2.3 Laboratory methods

DNA was extracted from samples using a salt extraction protocol (Sambrook and Russell, 2001), and 10,000ng per sample was sheared to approximately 200bp-500bp on a BioRuptor NGS (Diagenode) and dual-end size selected (0.8X-1.0X) with SPRI beads. Dual-indexed libraries were prepared from 375-2000ng of size selected DNA using KAPA LTP library prep kits (Glenn et al., 2017). These libraries were pooled (with samples from other projects) into batches of 16 samples at 250ng per sample (4,000ng total) and enriched in the presence of 30,000ng of c0t-1 repetitive sequence blocker (McCartney-Melstad et al., 2016) derived from *T. carnifex* (casualties from a removal action of an invasive population (Meilink et al., 2015)) by hybridizing blockers with libraries for 30 minutes and probes with libraries/blockers for 30 hours. Enriched libraries were subjected to 14 cycles of PCR with KAPA HiFi HotStart ReadyMix and pooled at an equimolar ratio for 150bp paired-end sequencing across multiple Illumina HiSeq 4000 lanes (receiving an aggregate of 18% of one lane, for a multiplexing equivalent of 128 samples per lane).

2.4 Processing of target capture data

A total of 3,937,346 read pairs from the sample receiving the greatest number of reads were used to *de novo* assemble target sequences for each target region using the assembly by reduced complexity (ARC) pipeline (Hunter et al., 2015). A single assembled contig was selected for each original target region by means of reciprocal best blast hit (RBBH) (Rivera et al., 1998), and these were used as a reference assembly for all downstream analyses. Adapter contamination was removed from sample reads using skewer v0.2.2 (Jiang et al., 2014), and reads were then mapped to the reference assembly using BWA-MEM v0.7.15-r1140 (Li, 2013). Picard tools v2.9.2 (https://broadinstitute.github.io/picard/) was used to add read group information and to mark PCR duplicates, and HaplotypeCaller and GenotypeGVCFs from GATK v3.8 (McKenna et al., 2010) were used jointly to genotype the relevant groups of

samples (either crested newts or crested newts + marbled newts depending on the analysis; see below). SNPs that failed any of the following hard filters were removed: QD < 2, MQ < 40, FS > 60, MQRankSum < -12.5, ReadPosRankSum < -8, and QUAL < 30 (Poplin et al., 2017). We next attempted to remove paralogous targets from our dataset with a Hardy Weinberg Equilibrium (HWE) filter for heterozygote excess. Heterozygote excess p-values were calculated for every SNP using vcftools 0.1.15 (Danecek et al., 2011), and any target containing at least one SNP with a heterozygote excess p-value < 0.05 was removed from downstream analysis. More detail on the processing of the target capture data can be found in Supplementary Text S2.

2.5 Phylogenetic analyses

A concatenated maximum likelihood phylogeny was inferred with RAxML version 8.2.11 (Stamatakis, 2014) based on an alignment of 133,601 SNPs across 5,866 different targets. We included all 23 *Triturus* individuals in this analysis. For gene-tree summary, ASTRAL v5.6.1 (Zhang et al., 2017) was used to estimate the crested newt species-tree from 5,610 gene-trees generated in RAxML. The 21 crested newt samples were assigned species membership, and no marbled newts were included because estimating terminal branch lengths is not possible for species with a single representative. For species-tree estimation, SNAPP v1.3.0 (Bryant et al., 2012) within the BEAST v2.4.8 (Bouckaert et al., 2014) environment was used to infer the crested newt species-tree from single biallelic SNPs randomly selected from each of 5,581 post-filtering targets. All three individuals per crested newt species were treated as a single terminal and marbled newts were again excluded given our single exemplar sampling of both species. We also estimated divergence times in SNAPP for the crested newts. The split between *T. carnifex* and *T. macedonicus*, assumed to correspond to the origin of the Adriatic Sea at the end of the Messinian Salinity Crisis 5.33 million years ago, was used as a single calibration

185 point (Arntzen et al., 2007; Wielstra and Arntzen, 2011) to produce a rough estimate of the
186 timing of cladogenesis. A detailed description of our strategy for phylogenetic analyses is
187 available in Supplementary Text S3.
188
189 **3. Results**
190 Samples received a mean of 2,812,980 read pairs (s.d. = 585,815). Enrichment was highly
191 efficient, especially given the large genome size of *Triturus*, with an average of 44.5% of raw
192 reads mapping to the assembled target sequences (s.d. = 2.6%). After removing PCR duplicates,
193 which accounted for an average of 22.6% of mapped reads, the unique read on target rate was
194 34.4% (s.d. = 1.9%). The 23 samples in the final RAxML alignment contained an average of
195 10.1% missing data (min = 3.2%, max = 31.8%) after setting genotype calls with GQ scores of
196 less than 20 to missing.
197 The concatenated analysis with RAxML supports a basal bifurcation in *Triturus* between
198 the marbled and crested newts (Fig. 3), consistent with the prevailing view that they are
199 reciprocally monophyletic (Arntzen et al., 2007; Espregueira Themudo et al., 2009; Wielstra
200 et al., 2014). RAxML also recovers each of the crested newt species as monophyletic,
201 validating our decision to collapse the three individuals sampled per species in a single terminal
202 in ASTRAL and SNAPP. Furthermore, all five *Triturus* body builds are recovered as
203 monophyletic (cf. Arntzen et al., 2007; Espregueira Themudo et al., 2009; Wielstra et al., 2014).
204 The greatest intraspecific divergence is observed in *T. carnifex* (Supplementary Text S1;
205 Supplementary Fig. S1; Supplementary Table S2).
206 Phylogenetic inference based on data concatenation with RAxML (Fig. 3), gene-tree
207 summary with ASTRAL (Fig. 4a) and species-tree estimation with SNAPP (Fig. 4b) all recover
208 the same crested newt topology, with a basal bifurcation between the *T. karelinii*-group (NTV
209 = 13; *T. ivanbureschi* as the sister taxon to *T. anatolicus* + *T. karelinii)* and the remaining taxa,

which themselves are resolved into the species pairs *T. carnifex* + *T. macedonicus* (NTV=14; the *T. carnifex*-group), and *T. cristatus* (NTV=15) + *T. dobrogicus* (NTV=16/17). Despite the rapidity of cladogenesis, we obtain strong branch support for every internal node. Even with the uncertainty in dating given a single biogeographically-derived calibration date, the bifurcation giving rise to the four crested newt species groups (cf. Fig. 1) must have occurred over a relatively short time frame (Fig. 5), reflected by two particularly short, but resolvable internal branches (Fig. 3; Fig. 4).

The phylogenomic analyses suggest considerable gene-tree/species-tree discordance in *Triturus*. The normalized quartet score of the ASTRAL tree (Fig. 4a), which reflects the proportion of input gene-tree quartets consistent with the species-tree, is 0.63, indicating a high degree of gene-tree discordance. Furthermore, the only node in the SNAPP tree with a posterior probability below 1.0 (i.e. 0.99) is subtended by a very short branch (Fig. 4b). Consistent with the high level of gene-tree/species-tree discordance, we also found that the full mtDNA-based phylogeny of *Triturus* produced a highly supported, but topologically different, phylogeny (Supplementary Text S3; Supplementary Fig. S2; Wielstra and Arntzen, 2011).

Considering an NTV count of 12, as observed in the marbled newts as well as the most closely related newt genera, as the ancestral state for *Triturus* (Arntzen et al., 2015; Veith et al., 2018), three sequential single-vertebral additions to NTV along internal branches, and one or two additions along the terminal branch leading to *T. dobrogicus* (in which NTV = 16 and NTV = 17 occur at approximately equal frequency; Arntzen et al., 2015; Wielstra et al., 2016) are required under a parsimony criterion (with either ACCTRAN or DELTRAN optimization) to explain the present-day variation in NTV observed in *Triturus* (Fig. 3). This is the minimum possible number of inferred changes in NTV count required to explain the NTV radiation observed today (Supplementary Fig. S3; Supplementary Text S5). No NTV deletions or

reversals are required, implying a linear, stepwise, single-addition scenario for NTV expansion in *Triturus*.

4. Discussion

We use a large, tramscriptome-derived phylogenomic dataset to construct a phylogenetic hypothesis and study the evolution of ecological and phenotypic diversity within the adaptive radiation of *Triturus* newts. In contrast to previous attempts to recover a multilocus species-tree (Arntzen et al., 2007; Espregueira Themudo et al., 2009; Wielstra et al., 2014), we recover full phylogenetic resolution with strong support across the tree. Despite cladogenesis having occurred in a relatively brief time window (Fig. 5), resulting in a high degree of gene-tree/species-tree discordance, independent phylogenetic approaches based on data concatenation (RAxML), gene-tree summarization (ASTRAL) and species-tree estimation (SNAPP), all recover the same, highly supported topology for *Triturus* (Fig. 3; Fig. 4). Our *Triturus* case study underscores that sequence capture by target enrichment is a promising approach to resolve the phylogenetic challenges associated with adaptive radiations, particularly for taxa with large and complicated genomes where other genomic approaches are impractical, including salamanders (McCartney-Melstad et al., 2016).

Our new phylogenetic hypothesis allows us to place the eco-morphological differentiation shown by *Triturus* into a coherent evolutionary context. Over time, *Triturus* expanded its range of NTV to encompass higher counts (Fig. 3). The *Triturus* tree is consistent with a maximally parsimonious scenario, under which four to five character state changes are required to explain the radiation in NTV observed today. Any other possible phylogenetic relationship among *Triturus* body builds would require a higher number of inferred NTV changes (Supplementary Fig. S3). Three of these inferred changes are positioned along internal branches, of which two are particularly short, suggesting that changes in NTV count can evolve

over a relatively short time. The fourth and fifth inferred change are situated on the external branch leading to *T. dobrogicus*, the only *Triturus* species with substantial intraspecific variation in NTV count (Arntzen et al., 2015; Wielstra et al., 2016).

Newts annually alternate between an aquatic and a terrestrial habitat, and the functional trade-off between adaptation to life in water or on land likely poses contrasting demands on body build (Fish and Baudinette, 1999; Gillis and Blob, 2001; Gvoždík and van Damme, 2006; Shine and Shetty, 2001). Considering the observed relationship between one additional trunk vertebra and an extra month annually spent in the water (Fig. 1), the extraordinary NTV variation observed in *Triturus* may reflect the morphological mechanism by which more efficient exploitation of a wider range in hydroperiod (i.e. the annual availability of standing water) evolved. Despite the evolvability of NTV count (Arntzen et al., 2015), NTV evolution has been phylogenetically constrained in *Triturus*. Apparently the change in NTV was directional and involved the addition of a single trunk vertebra at a time (Fig. 3; Supplementary Fig. S3). Species with a more derived body build, reflected in a higher NTV, have a relatively prolonged aquatic period and, because species with transitional NTV counts remain extant, the end result is an eco-morphological radiation.

Triturus newts show a slight degree of intraspecific variation in NTV today. Such variation is partially explained by interspecific hybridization (emphasizing the genetic basis of NTV count; Arntzen et al., 2014), but there is standing variation in NTV count within all *Triturus* species (Slijepčević et al., 2015). This suggests that, during *Triturus* evolution, there has always been intraspecific NTV count polymorphism that could be subjected to natural selection. Whether there is a causal relationship between the directional, parsimonious evolution of higher NTV and the equally parsimonious evolutionary increase in aquatic lifestyle, and, if so, which of these two may be the actual target of selection, remain important open questions. A proper understanding of the functional relationship between NTV, body

build and fitness in aquatic/terrestrial environments in *Triturus* is still lacking (Gvoždík and van Damme, 2006), and functional studies exploring this fitness landscape across intra and interspecific variation in NTV is an important next step in establishing a firm causal relationship between variation, performance and fitness. The recent availability of the first salamander genomes (Elewa et al., 2017; Nowoshilow et al., 2018; Smith et al., 2018) finally offers the prospect of sequencing the genome of each *Triturus* species and exploring the developmental basis for NTV and its functional consequences in the diversification of the genus.

Acknowledgements

Andrea Chiocchio, Daniele Canestrelli, Michael Fahrbach, Ana Ivanović, Raymond van der Lans, and Kurtuluş Olgun helped obtain samples for transcriptome sequencing. Permits were provided by the Italian Ministry of the Environment (DPN-2009-0026530), the Environment Protection Agency of Montenegro (no. UPI-328/4), the Ministry of Energy, Development and Environmental Protection of Republic of Serbia (no. 353-01-75/2014-08), and TÜBİTAK, Turkey (no. 113Z752). RAVON & Natuurbalans-Limes Divergens provided the *T. carnifex* used to create c0t-1. Tara Luckau helped in the lab. Peter Scott provided valuable suggestions on methodology. Wiesław Babik and Ana Ivanović commented on an earlier version of this manuscript. This work used the Vincent J. Coates Genomics Sequencing Laboratory at UC Berkeley, supported by NIH S10 Instrumentation Grants S10RR029668 and S10RR027303. Computing resources were provided by XSEDE (Towns et al., 2014) and the Texas Advanced Computing Center (TACC) Stampede2 cluster at The University of Texas at Austin.

Funding

This project has received funding from the European Union's Horizon 2020 research and innovation programme under the Marie Skłodowska-Curie grant agreement No. 655487.

Data availability

Raw sequence read data for the sequence capture libraries of the 23 *Triturus* samples and the 12 transcriptome libraries are available at SRA (PRJNA498336). Transcriptome assemblies, genotype calls (VCF) for the 21- and 23-sample datasets, input files for the RAxML, ASTRAL and SNAPP analyses, and synthesized target sequences are available at Zenodo (https://doi.org/10.5281/zenodo.1470914). Supplementary data associated with this article can be found, in the online version, at https://doi.org/10.1016/j.ympev.2018.12.032.

References

Abdelkrim, J., Aznar-Cormano, L., Fedosov, A., Kantor, Y., Lozouet, P., Phuong, M., Zaharias, P., Puillandre, N., 2018. Exon-capture based phylogeny and diversification of the venomous gastropods (Neogastropoda, Conoidea). Mol. Biol. Evol. 35, 2355–2374.

Alföldi, J., Di Palma, F., Grabherr, M., Williams, C., Kong, L., Mauceli, E., Russell, P., Lowe, C.B., Glor, R.E., Jaffe, J.D., Ray, D.A., Boissinot, S., Shedlock, A.M., Botka, C., Castoe, T.A., Colbourne, J.K., Fujita, M.K., Moreno, R.G., ten Hallers, B.F., Haussler, D., Heger, A., Heiman, D., Janes, D.E., Johnson, J., de Jong, P.J., Koriabine, M.Y., Lara, M., Novick, P.A., Organ, C.L., Peach, S.E., Poe, S., Pollock, D.D., de Queiroz, K., Sanger, T., Searle, S., Smith, J.D., Smith, Z., Swofford, R., Turner-Maier, J., Wade, J., Young, S., Zadissa, A., Edwards, S.V., Glenn, T.C., Schneider, C.J., Losos, J.B., Lander, E.S., Breen, M., Ponting, C.P., Lindblad-Toh, K., 2011. The genome of the green anole lizard and a comparative analysis with birds and mammals. Nature 477, 587.

Arntzen, J.W., 2003. *Triturus cristatus* Superspecies - Kammolch-Artenkreis (*Triturus cristatus* (Laurenti, 1768) - Nördlicher Kammolch, *Triturus carnifex* (Laurenti, 1768) - Italienischer Kammolch, *Triturus dobrogicus* (Kiritzescu, 1903) - Donau-Kammolch, *Triturus karelinii* (Strauch, 1870) - Südlicher Kammolch). In: Grossenbacher, K., Thiesmeier, B. (Eds.), Handbuch der Reptilien und Amphibien Europas. Schwanzlurche IIA. Aula-Verlag, Wiebelsheim, pp. 421-514.

Arntzen, J.W., Beukema, W., Galis, F., Ivanović, A., 2015. Vertebral number is highly evolvable in salamanders and newts (family Salamandridae) and variably associated with climatic parameters. Contrib. Zool. 84, 85-113.

Arntzen, J.W., Espregueira Themudo, G., Wielstra, B., 2007. The phylogeny of crested newts (*Triturus cristatus* superspecies): nuclear and mitochondrial genetic characters suggest a hard polytomy, in line with the paleogeography of the centre of origin. Contrib. Zool. 76, 261-278.

Arntzen, J.W., Wallis, G.P., 1999. Geographic variation and taxonomy of crested newts (*Triturus cristatus* superspecies): morphological and mitochondrial data. Contrib. Zool. 68, 181-203.

Arntzen, J.W., Wielstra, B., Wallis, G.P., 2014. The modality of nine *Triturus* newt hybrid zones, assessed with nuclear, mitochondrial and morphological data. Biol. J. Linn. Soc. 113, 604–622.

Bi, K., Vanderpool, D., Singhal, S., Linderoth, T., Moritz, C., Good, J.M., 2012. Transcriptome-based exon capture enables highly cost-effective comparative genomic data collection at moderate evolutionary scales. BMC Genomics 13, 403.

Bork, P., Dandekar, T., Diaz-Lazcoz, Y., Eisenhaber, F., Huynen, M., Yuan, Y., 1998. Predicting function: from genes to genomes and back. J. Mol. Biol. 283, 707-725.

Bouckaert, R., Heled, J., Kühnert, D., Vaughan, T., Wu, C.-H., Xie, D., Suchard, M.A., Rambaut, A., Drummond, A.J., 2014. BEAST 2: a software platform for Bayesian evolutionary analysis. PLoS Comput. Biol. 10, e1003537.

Bragg, J.G., Potter, S., Bi, K., Moritz, C., 2016. Exon capture phylogenomics: efficacy across scales of divergence. Mol. Ecol. Resour. 16, 1059-1068.

Bryant, D., Bouckaert, R., Felsenstein, J., Rosenberg, N.A., RoyChoudhury, A., 2012. Inferring species trees directly from biallelic genetic markers: bypassing gene trees in a full coalescent analysis. Mol. Biol. Evol. 29, 1917-1932.

Camacho, C., Coulouris, G., Avagyan, V., Ma, N., Papadopoulos, J., Bealer, K., Madden, T.L., 2009. BLAST+: architecture and applications. BMC Bioinformatics 10, 421-421.

Crawford, N.G., Faircloth, B.C., McCormack, J.E., Brumfield, R.T., Winker, K., Glenn, T.C., 2012. More than 1000 ultraconserved elements provide evidence that turtles are the sister group of archosaurs. Biol. Lett. 8, 783-786.

Danecek, P., Auton, A., Abecasis, G., Albers, C.A., Banks, E., DePristo, M.A., Handsaker, R.E., Lunter, G., Marth, G.T., Sherry, S.T., McVean, G., Durbin, R., Genomes Project Analysis, G., 2011. The variant call format and VCFtools. Bioinformatics 27, 2156-2158.

Degnan, J.H., Rosenberg, N.A., 2006. Discordance of species trees with their most likely gene trees. PLoS Genet. 2, e68.

Edgar, R.C., 2010. Search and clustering orders of magnitude faster than BLAST. Bioinformatics 26, 2460-2461.

Elewa, A., Wang, H., Talavera-López, C., Joven, A., Brito, G., Kumar, A., Hameed, L.S., Penrad-Mobayed, M., Yao, Z., Zamani, N., Abbas, Y., Abdullayev, I., Sandberg, R., Grabherr, M., Andersson, B., Simon, A., 2017. Reading and editing the *Pleurodeles waltl* genome reveals novel features of tetrapod regeneration. Nat. Commun. 8, 2286.

379 Espregueira Themudo, G., Wielstra, B., Arntzen, J.W., 2009. Multiple nuclear and
380 mitochondrial genes resolve the branching order of a rapid radiation of crested newts (*Triturus*,
381 Salamandridae). Mol. Phylogenet. Evol. 52, 321-328.

382 Felsenstein, J., 1978. Cases in which parsimony or compatibility methods will be positively
383 misleading. Syst. Biol. 27, 401-410.

384 Fish, F.E., Baudinette, R.V., 1999. Energetics of locomotion by the Australian water rat
385 (*Hydromys chrysogaster*): a comparison of swimming and running in a semi-aquatic mammal.
386 The Journal of Experimental Biology 202, 353.

387 Giarla, T.C., Esselstyn, J.A., 2015. The challenges of resolving a rapid, recent radiation:
388 empirical and simulated phylogenomics of Philippine shrews. Syst. Biol. 64, 727-740.

389 Gillis, G.B., Blob, R.W., 2001. How muscles accommodate movement in different physical
390 environments: aquatic vs. terrestrial locomotion in vertebrates. Comparative Biochemistry and
391 Physiology Part A: Molecular & Integrative Physiology 131, 61-75.

392 Glenn, T.C., Bayona-Vásquez, N.J., Kieran, T.J., Pierson, T.W., Hoffberg, S.L., Scott, P.A.,
393 Louha, S., Bentley, K.E., Finger Jr., J.W., Troendle, N., Díaz-Jaimes, P., Mauricio, R.,
394 Faircloth, B.C., 2017. Adapterama III: Quadruple-indexed, triple-enzyme RADseq libraries
395 for about $1USD per Sample (3RAD). BioRxiv.

396 Gnirke, A., Melnikov, A., Maguire, J., Rogov, P., LeProust, E.M., Brockman, W., Fennell, T.,
397 Giannoukos, G., Fisher, S., Russ, C., Gabriel, S., Jaffe, D.B., Lander, E.S., Nusbaum, C., 2009.
398 Solution hybrid selection with ultra-long oligonucleotides for massively parallel targeted
399 sequencing. Nat. Biotechnol. 27, 182.

400 Govedarica, P., Cvijanović, M., Slijepčević, M., Ivanović, A., 2017. Trunk elongation and
401 ontogenetic changes in the axial skeleton of *Triturus* newts. J. Morphol. 278, 1577-1585.

402 Grabherr, M.G., Haas, B.J., Yassour, M., Levin, J.Z., Thompson, D.A., Amit, I., Adiconis, X.,
403 Fan, L., Raychowdhury, R., Zeng, Q., Chen, Z., Mauceli, E., Hacohen, N., Gnirke, A., Rhind,
404 N., di Palma, F., Birren, B.W., Nusbaum, C., Lindblad-Toh, K., Friedman, N., Regev, A., 2011.
405 Full-length transcriptome assembly from RNA-Seq data without a reference genome. Nat.
406 Biotechnol. 29, 644-652.

407 Gvoždík, L., van Damme, R., 2006. *Triturus* newts defy the running-swimming dilemma.
408 Evolution 60, 2110-2121.

409 Hammond, S.A., Warren, R.L., Vandervalk, B.P., Kucuk, E., Khan, H., Gibb, E.A., Pandoh,
410 P., Kirk, H., Zhao, Y., Jones, M., Mungall, A.J., Coope, R., Pleasance, S., Moore, R.A., Holt,
411 R.A., Round, J.M., Ohora, S., Walle, B.V., Veldhoen, N., Helbing, C.C., Birol, I., 2017. The
412 North American bullfrog draft genome provides insight into hormonal regulation of long
413 noncoding RNA. Nat. Commun. 8, 1433.

414 Hellsten, U., Harland, R.M., Gilchrist, M.J., Hendrix, D., Jurka, J., Kapitonov, V., Ovcharenko,
415 I., Putnam, N.H., Shu, S., Taher, L., Blitz, I.L., Blumberg, B., Dichmann, D.S., Dubchak, I.,
416 Amaya, E., Detter, J.C., Fletcher, R., Gerhard, D.S., Goodstein, D., Graves, T., Grigoriev, I.V.,
417 Grimwood, J., Kawashima, T., Lindquist, E., Lucas, S.M., Mead, P.E., Mitros, T., Ogino, H.,
418 Ohta, Y., Poliakov, A.V., Pollet, N., Robert, J., Salamov, A., Sater, A.K., Schmutz, J., Terry,
419 A., Vize, P.D., Warren, W.C., Wells, D., Wills, A., Wilson, R.K., Zimmerman, L.B., Zorn,

A.M., Grainger, R., Grammer, T., Khokha, M.K., Richardson, P.M., Rokhsar, D.S., 2010. The genome of the western clawed frog *Xenopus tropicalis*. Science 328, 633.

Hunter, S.S., Lyon, R.T., Sarver, B.A.J., Hardwick, K., Forney, L.J., Settles, M.L., 2015. Assembly by Reduced Complexity (ARC): a hybrid approach for targeted assembly of homologous sequences. bioRxiv.

Irisarri, I., Meyer, A., 2016. The identification of the closest living relative(s) of tetrapods: phylogenomic lessons for resolving short ancient internodes. Syst. Biol. 65, 1057-1075.

Jarvis, E.D., Mirarab, S., Aberer, A.J., Li, B., Houde, P., Li, C., Ho, S.Y.W., Faircloth, B.C., Nabholz, B., Howard, J.T., Suh, A., Weber, C.C., da Fonseca, R.R., Li, J., Zhang, F., Li, H., Zhou, L., Narula, N., Liu, L., Ganapathy, G., Boussau, B., Bayzid, M.S., Zavidovych, V., Subramanian, S., Gabaldón, T., Capella-Gutiérrez, S., Huerta-Cepas, J., Rekepalli, B., Munch, K., Schierup, M., Lindow, B., Warren, W.C., Ray, D., Green, R.E., Bruford, M.W., Zhan, X., Dixon, A., Li, S., Li, N., Huang, Y., Derryberry, E.P., Bertelsen, M.F., Sheldon, F.H., Brumfield, R.T., Mello, C.V., Lovell, P.V., Wirthlin, M., Schneider, M.P.C., Prosdocimi, F., Samaniego, J.A., Velazquez, A.M.V., Alfaro-Núñez, A., Campos, P.F., Petersen, B., Sicheritz-Ponten, T., Pas, A., Bailey, T., Scofield, P., Bunce, M., Lambert, D.M., Zhou, Q., Perelman, P., Driskell, A.C., Shapiro, B., Xiong, Z., Zeng, Y., Liu, S., Li, Z., Liu, B., Wu, K., Xiao, J., Yinqi, X., Zheng, Q., Zhang, Y., Yang, H., Wang, J., Smeds, L., Rheindt, F.E., Braun, M., Fjeldsa, J., Orlando, L., Barker, F.K., Jønsson, K.A., Johnson, W., Koepfli, K.-P., O'Brien, S., Haussler, D., Ryder, O.A., Rahbek, C., Willerslev, E., Graves, G.R., Glenn, T.C., McCormack, J., Burt, D., Ellegren, H., Alström, P., Edwards, S.V., Stamatakis, A., Mindell, D.P., Cracraft, J., Braun, E.L., Warnow, T., Jun, W., Gilbert, M.T.P., Zhang, G., 2014. Whole-genome analyses resolve early branches in the tree of life of modern birds. Science 346, 1320.

Jiang, H., Lei, R., Ding, S.-W., Zhu, S., 2014. Skewer: a fast and accurate adapter trimmer for next-generation sequencing paired-end reads. BMC Bioinformatics 15, 182.

Kutschera, V.E., Bidon, T., Hailer, F., Rodi, J.L., Fain, S.R., Janke, A., 2014. Bears in a forest of gene trees: phylogenetic inference is complicated by incomplete lineage sorting and gene flow. Mol. Biol. Evol. 31, 2004-2017.

Lanza, B., Arntzen, J.W., Gentile, E., 2010. Vertebral numbers in the Caudata of the Western Palearctic (Amphibia). Atti Mus. Civ. Stor. Nat. Trieste 54, 3-114.

Leaché, A.D., Banbury, B.L., Linkem, C.W., de Oca, A.N.-M., 2016. Phylogenomics of a rapid radiation: is chromosomal evolution linked to increased diversification in north american spiny lizards (Genus Sceloporus)? BMC Evol. Biol. 16, 63.

Leaché, A.D., Harris, R.B., Rannala, B., Yang, Z., 2014. The influence of gene flow on species tree estimation: a simulation study. Syst. Biol. 63, 17-30.

Léveillé-Bourret, É., Starr, J.R., Ford, B.A., Moriarty Lemmon, E., Lemmon, A.R., 2018. Resolving rapid radiations within angiosperm families using anchored phylogenomics. Syst. Biol. 67, 94-112.

Li, H., 2013. Aligning sequence reads, clone sequences and assembly contigs with BWA-MEM. arXiv preprint arXiv:1303.3997.

460 Mallet, J., Besansky, N., Hahn, M.W., 2016. How reticulated are species? Bioessays 38, 140-
461 149.

462 McCartney-Melstad, E., Mount, G.G., Bradley Shaffer, H., 2016. Exon capture optimization
463 in amphibians with large genomes. Mol. Ecol. Resour. 16, 1084-1094.

464 McCartney-Melstad, E., Vu, J.K., Shaffer, H.B., 2018. Genomic data recover previously
465 undetectable fragmentation effects in an endangered amphibian. Mol. Ecol.,
466 https://doi.org/10.1111/mec.14892.

467 McCormack, J.E., Faircloth, B.C., Crawford, N.G., Gowaty, P.A., Brumfield, R.T., Glenn, T.C.,
468 2012. Ultraconserved elements are novel phylogenomic markers that resolve placental
469 mammal phylogeny when combined with species-tree analysis. Genome Res. 22, 746-754.

470 McKenna, A., Hanna, M., Banks, E., Sivachenko, A., Cibulskis, K., Kernytsky, A., Garimella,
471 K., Altshuler, D., Gabriel, S., Daly, M., DePristo, M.A., 2010. The Genome Analysis Toolkit:
472 A MapReduce framework for analyzing next-generation DNA sequencing data. Genome Res.
473 20, 1297-1303.

474 Meiklejohn, K.A., Faircloth, B.C., Glenn, T.C., Kimball, R.T., Braun, E.L., 2016. Analysis of
475 a rapid evolutionary radiation using ultraconserved elements: evidence for a bias in some
476 multispecies coalescent methods. Syst. Biol. 65, 612-627.

477 Meilink, W.R.M., Arntzen, J.W., van Delft, J.J.C.W., Wielstra, B., 2015. Genetic pollution of
478 a threatened native crested newt species through hybridization with an invasive congener in the
479 Netherlands. Biol. Conserv. 184, 145-153.

480 Nater, A., Burri, R., Kawakami, T., Smeds, L., Ellegren, H., 2015. Resolving evolutionary
481 relationships in closely related species with whole-genome sequencing data. Syst. Biol. 64,
482 1000-1017.

483 Neves, L.G., Davis, J.M., Barbazuk, W.B., Kirst, M., 2013. Whole-exome targeted sequencing
484 of the uncharacterized pine genome. The Plant Journal 75, 146-156.

485 Nowoshilow, S., Schloissnig, S., Fei, J.-F., Dahl, A., Pang, A.W.C., Pippel, M., Winkler, S.,
486 Hastie, A.R., Young, G., Roscito, J.G., Falcon, F., Knapp, D., Powell, S., Cruz, A., Cao, H.,
487 Habermann, B., Hiller, M., Tanaka, E.M., Myers, E.W., 2018. The axolotl genome and the
488 evolution of key tissue formation regulators. Nature 554, 50-55.

489 Pamilo, P., Nei, M., 1988. Relationships between gene trees and species trees. Mol. Biol. Evol.
490 5, 568-583.

491 Philippe, H., Brinkmann, H., Lavrov, D.V., Littlewood, D.T.J., Manuel, M., Wörheide, G.,
492 Baurain, D., 2011. Resolving difficult phylogenetic questions: why more sequences are not
493 enough. PLoS Biol. 9, e1000602.

494 Pollard, D.A., Iyer, V.N., Moses, A.M., Eisen, M.B., 2006. Widespread discordance of gene
495 trees with species tree in *Drosophila*: evidence for incomplete lineage sorting. PLoS Genet. 2,
496 e173.

497 Poplin, R., Ruano-Rubio, V., DePristo, M.A., Fennell, T.J., Carneiro, M.O., Van der Auwera,
498 G.A., Kling, D.E., Gauthier, L.D., Levy-Moonshine, A., Roazen, D., Shakir, K., Thibault, J.,

Chandran, S., Whelan, C., Lek, M., Gabriel, S., Daly, M.J., Neale, B., MacArthur, D.G., Banks, E., 2017. Scaling accurate genetic variant discovery to tens of thousands of samples. bioRxiv.

Rivera, M.C., Jain, R., Moore, J.E., Lake, J.A., 1998. Genomic evidence for two functionally distinct gene classes. Proc. Natl. Acad. Sci. U.S.A. 95, 6239-6244.

Sambrook, J., Russell, D.W., 2001. Molecular cloning: a laboratory manual 3rd edition. Coldspring-Harbour Laboratory Press, UK.

Scott, P.A., Glenn, T.C., Rissler, L.J., 2018. Resolving taxonomic turbulence and uncovering cryptic diversity in the musk turtles (*Sternotherus*) using robust demographic modeling. Mol. Phylogenet. Evol. 120, 1-15.

Shaffer, H.B., Minx, P., Warren, D.E., Shedlock, A.M., Thomson, R.C., Valenzuela, N., Abramyan, J., Amemiya, C.T., Badenhorst, D., Biggar, K.K., Borchert, G.M., Botka, C.W., Bowden, R.M., Braun, E.L., Bronikowski, A.M., Bruneau, B.G., Buck, L.T., Capel, B., Castoe, T.A., Czerwinski, M., Delehaunty, K.D., Edwards, S.V., Fronick, C.C., Fujita, M.K., Fulton, L., Graves, T.A., Green, R.E., Haerty, W., Hariharan, R., Hernandez, O., Hillier, L.W., Holloway, A.K., Janes, D., Janzen, F.J., Kandoth, C., Kong, L., de Koning, A.J., Li, Y., Literman, R., McGaugh, S.E., Mork, L., O'Laughlin, M., Paitz, R.T., Pollock, D.D., Ponting, C.P., Radhakrishnan, S., Raney, B.J., Richman, J.M., St John, J., Schwartz, T., Sethuraman, A., Spinks, P.Q., Storey, K.B., Thane, N., Vinar, T., Zimmerman, L.M., Warren, W.C., Mardis, E.R., Wilson, R.K., 2013. The western painted turtle genome, a model for the evolution of extreme physiological adaptations in a slowly evolving lineage. Genome Biol. 14, R28.

Shi, C.-M., Yang, Z., 2018. Coalescent-based analyses of genomic sequence data provide a robust resolution of phylogenetic relationships among major groups of gibbons. Mol. Biol. Evol. 35, 159-179.

Shine, R., Shetty, S., 2001. Moving in two worlds: aquatic and terrestrial locomotion in sea snakes (*Laticauda colubrina*, Laticaudidae). J. Evol. Biol. 14, 338-346.

Slijepčević, M., Galis, F., Arntzen, J.W., Ivanović, A., 2015. Homeotic transformations and number changes in the vertebral column of *Triturus* newts. PeerJ 3, e1397.

Smith, J.J., Timoshevskaya, N., Timoshevskiy, V.A., Keinath, M.C., Hardy, D., Voss, S.R., 2018. A chromosome-scale assembly of the enormous (32 Gb) *Axolotl* genome. bioRxiv.

Song, S., Liu, L., Edwards, S.V., Wu, S., 2012. Resolving conflict in eutherian mammal phylogeny using phylogenomics and the multispecies coalescent model. Proc. Natl. Acad. Sci. U.S.A. 109, 14942-14947.

Spinks, P.Q., Thomson, R.C., Pauly, G.B., Newman, C.E., Mount, G., Shaffer, H.B., 2013. Misleading phylogenetic inferences based on single-exemplar sampling in the turtle genus *Pseudemys*. Mol. Phylogenet. Evol. 68, 269-281.

Stamatakis, A., 2014. RAxML version 8: a tool for phylogenetic analysis and post-analysis of large phylogenies. Bioinformatics 30, 1312-1313.

Stroud, J.T., Losos, J.B., 2016. Ecological opportunity and adaptive radiation. Annu. Rev. Ecol. Evol. Syst. 47, 507-532.

Sun, Y.-B., Xiong, Z.-J., Xiang, X.-Y., Liu, S.-P., Zhou, W.-W., Tu, X.-L., Zhong, L., Wang, L., Wu, D.-D., Zhang, B.-L., Zhu, C.-L., Yang, M.-M., Chen, H.-M., Li, F., Zhou, L., Feng, S.-H., Huang, C., Zhang, G.-J., Irwin, D., Hillis, D.M., Murphy, R.W., Yang, H.-M., Che, J., Wang, J., Zhang, Y.-P., 2015. Whole-genome sequence of the Tibetan frog *Nanorana parkeri* and the comparative evolution of tetrapod genomes. Proc. Natl. Acad. Sci. U.S.A. 112, E1257.

Swofford, D.L., Waddell, P.J., Huelsenbeck, J.P., Foster, P.G., Lewis, P.O., Rogers, J.S., 2001. Bias in phylogenetic estimation and Its relevance to the choice between parsimony and likelihood methods. Syst. Biol. 50, 525-539.

Tatusov, R.L., Koonin, E.V., Lipman, D.J., 1997. A genomic perspective on protein families. Science 278, 631.

Towns, J., Cockerill, T., Dahan, M., Foster, I., Gaither, K., Grimshaw, A., Hazlewood, V., Lathrop, S., Lifka, D., Peterson, G.D., Roskies, R., Scott, J.R., Wilkins-Diehr, N., 2014. XSEDE: accelerating acientific discovery. Computing in Science & Engineering 16, 62-74.

Urošević, A., Slijepčević, M.D., Arntzen, J.W., Ivanović, A., 2016. Vertebral shape and body elongation in *Triturus* newts. Zoology 119, 439-446.

Veith, M., Bogaerts, S., Pasmans, F., Kieren, S., 2018. The changing views on the evolutionary relationships of extant Salamandridae (Amphibia: Urodela). PLoS ONE 13, e0198237.

Vukov, T.D., Sotiropoulos, K., Wielstra, B., Džukić, G., Kalezić, M.L., 2011. The evolution of the adult body form of the crested newt (*Triturus cristatus* superspecies, Caudata, Salamandridae). Journal of Zoological Systematics and Evolutionary Research 49, 324-334.

Whitfield, J.B., Lockhart, P.J., 2007. Deciphering ancient rapid radiations. Trends Ecol. Evol. 22, 258-265.

Wielstra, B., Arntzen, J.W., 2011. Unraveling the rapid radiation of crested newts (*Triturus cristatus* superspecies) using complete mitogenomic sequences. BMC Evol. Biol. 11, 162.

Wielstra, B., Arntzen, J.W., van der Gaag, K., Pabijan, M., Babik, W., 2014. Data concatenation, Bayesian concordance and coalescent-based analyses of the species tree for the rapid radiation of *Triturus* newts. PLoS ONE 9, e111011.

Wielstra, B., Burke, T., Butlin, R.K., Arntzen, J.W., 2017a. A signature of dynamic biogeography: enclaves indicate past species replacement. Proc. Royal Soc. B 284, 20172014.

Wielstra, B., Burke, T., Butlin, R.K., Avcı, A., Üzüm, N., Bozkurt, E., Olgun, K., Arntzen, J.W., 2017b. A genomic footprint of hybrid zone movement in crested newts. Evolution Letters 1, 93-101.

Wielstra, B., Crnobrnja-Isailović, J., Litvinchuk, S.N., Reijnen, B.T., Skidmore, A.K., Sotiropoulis, K., Toxopeus, A.G., Tzankov, N., Vukov, T., Arntzen, J.W., 2013. Tracing glacial refugia of *Triturus* newts based on mitochondrial DNA phylogeography and species distribution modeling. Front. Zool. 10, 13.

Wielstra, B., Vörös, J., Arntzen, J.W., 2016. Is the Danube crested newt *Triturus dobrogicus* polytypic? A review and new nuclear DNA data. Amphib.-Reptil. 37, 167-177.

576 Zhang, C., Sayyari, E., Mirarab, S., 2017. ASTRAL-III: Increased Scalability and Impacts of
577 Contracting Low Support Branches. In: Meidanis, J., Nakhleh, L. (Eds.), Comparative
578 Genomics. Springer International Publishing, Cham, pp. 53-75.

579

580 **Figures**

581

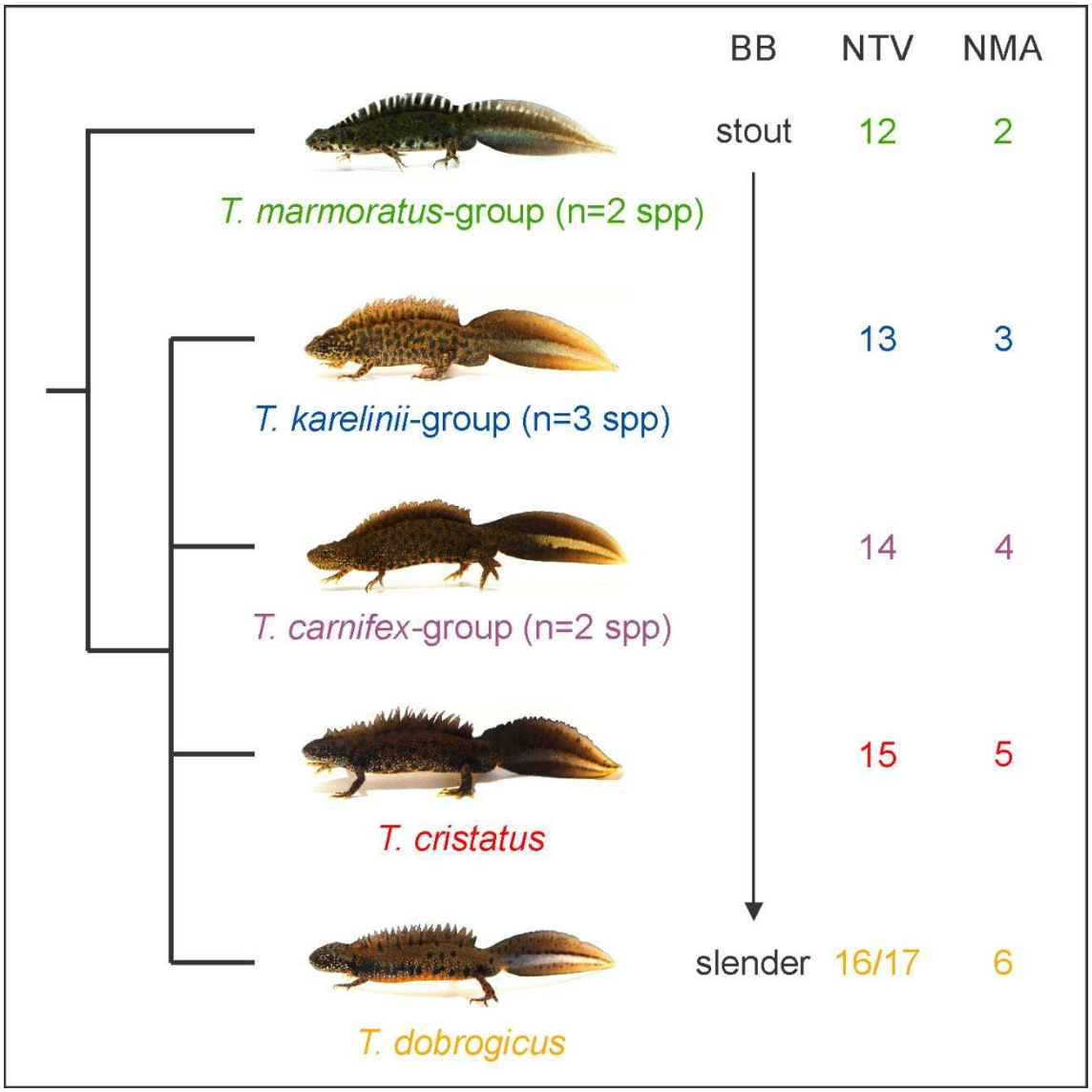

582

583 **Fig. 1. The adaptive radiation of *Triturus* newts.** Five body builds (BB) from stout to slender
584 are observed in *Triturus* that are also characterized by an increasing number of trunk vertebrae
585 (NTV) and number of annual aquatic months (NMA). The marbled newts (*T. marmoratus*-
586 group) and crested newts (remaining four BBs) are sister clades. Relationships among the
587 crested newts are not yet resolved and are the main focus of the present study.

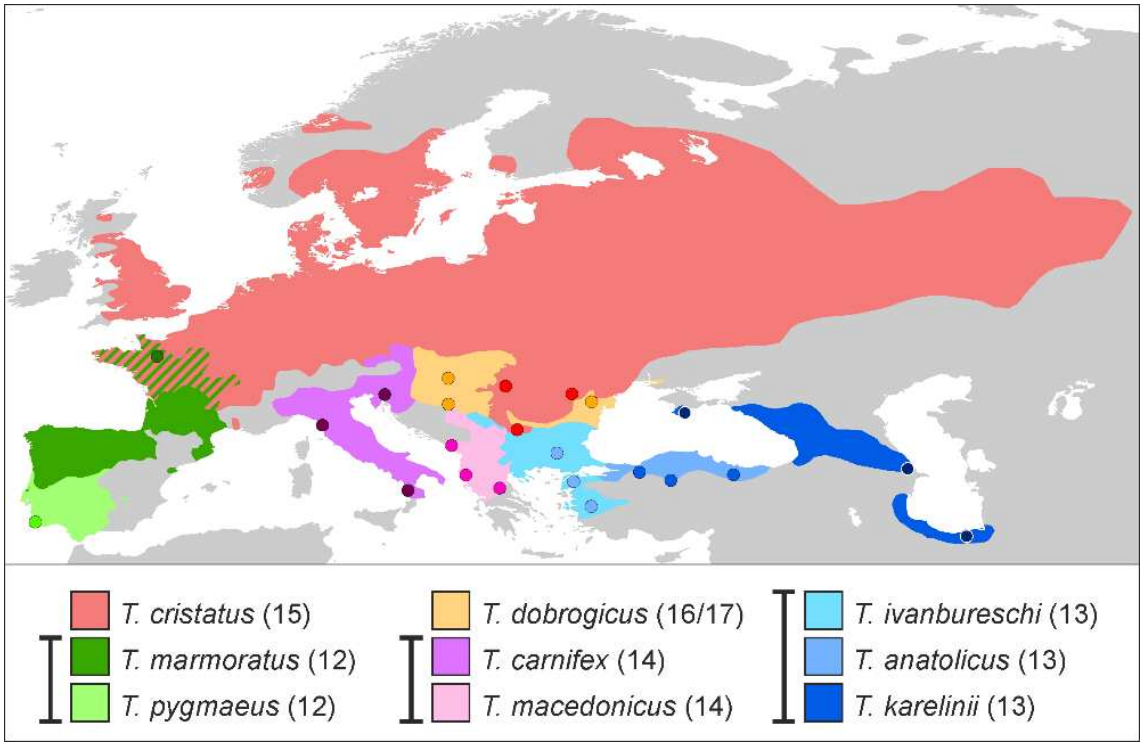

588

589 **Fig. 2. Distribution and sampling scheme for *Triturus*.** Dots represent sample localities
590 (details in Supplementary Table S1). For the marbled newts (in green) a single individual is
591 sampled for each of the two species and for the crested newts (other colours) three individuals
592 are sampled for all seven species. The number in parentheses reflects each species'
593 characteristic number of trunk vertebrae and whiskers link species that possess the same body
594 build (see Fig. 1).

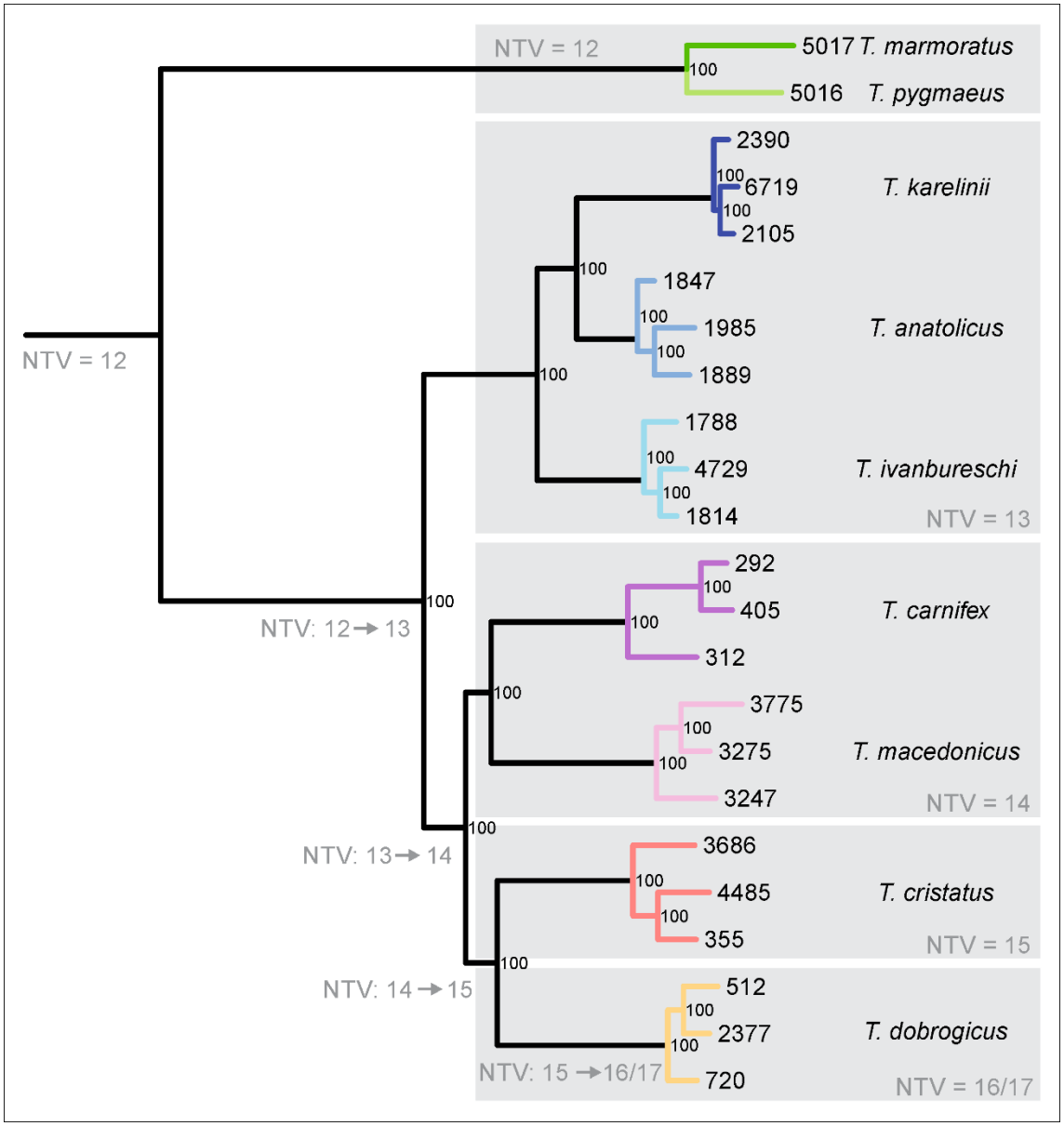

595

596 **Fig. 3. *Triturus* newt phylogeny based on data concatenation with RAxML.** This maximum
597 likelihood phylogeny is based on 133,601 SNPs derived from 5,866 nuclear markers. Numbers
598 at nodes indicate bootstrap support from 100 rapid bootstrap replicates. The five *Triturus* body
599 builds (see Fig. 1) are delineated by grey boxes, with their characteristic number of trunk
600 vertebrae (NTV) noted. Inferred changes in NTV under the parsimony criterion are noted along
601 branches. Colours reflect species and correspond to Fig. 2. Tip labels correspond to
602 Supplementary Table S1.

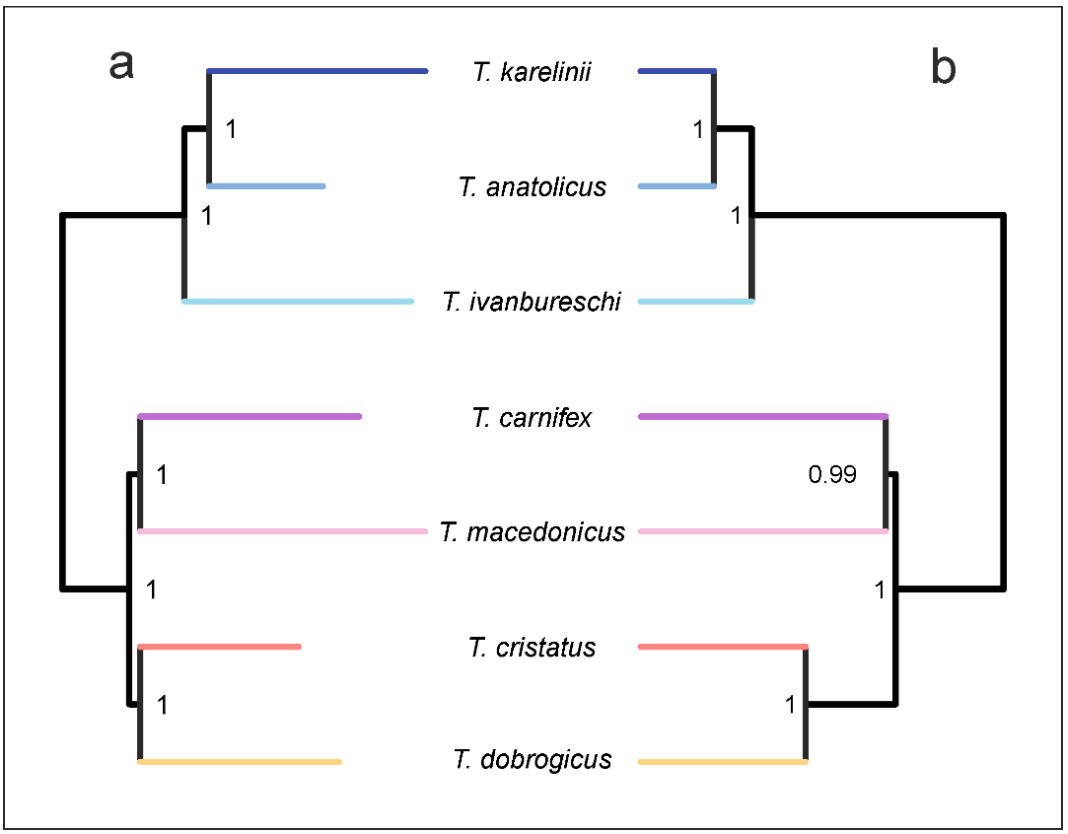

603

604 **Fig. 4. Crested newt phylogeny based on gene-tree summary with ASTRAL and species-**
605 **tree estimation with SNAPP.** The ASTRAL tree (a) is based on 5,610 gene-trees. Numbers
606 at nodes indicate local quartet support posterior probabilities. The SNAPP tree (b) is based on
607 single biallelic SNPs taken from 5,581 nuclear markers. Numbers at nodes indicate posterior
608 probabilities. Colours reflect species and correspond to Fig. 2. Note that both topologies are
609 identical to the phylogeny based on data concatenation (Fig. 3).

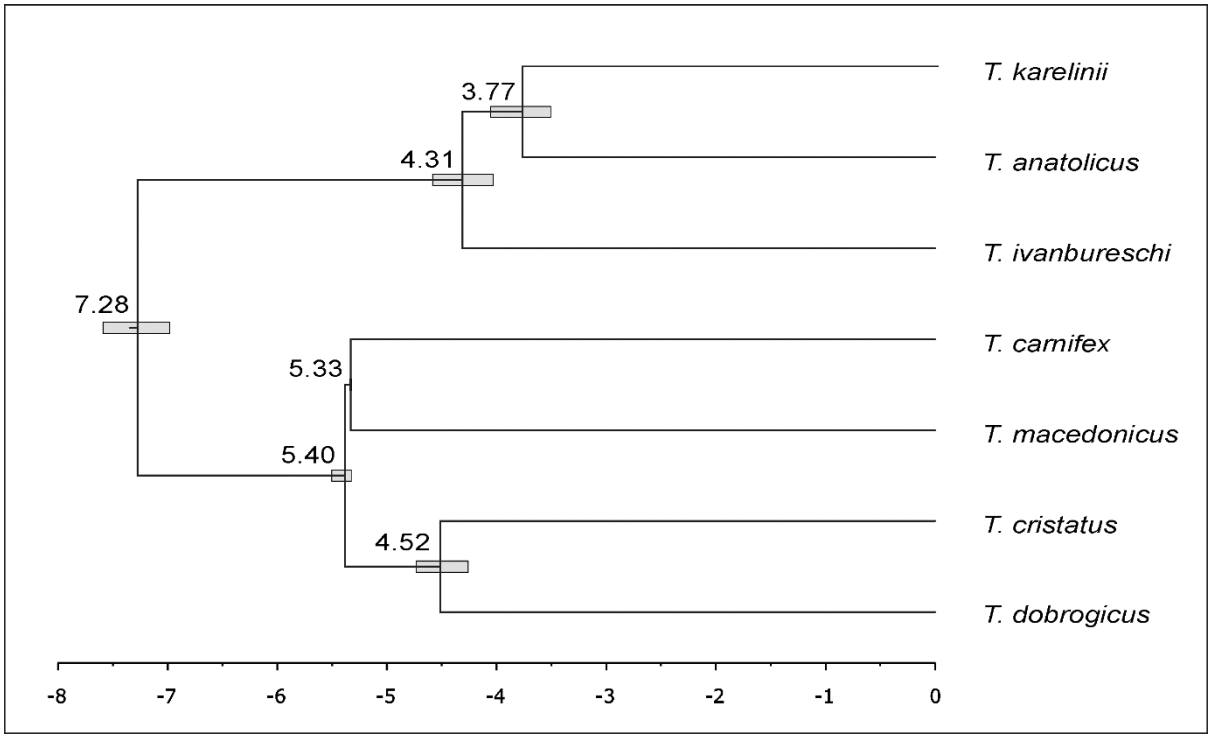

Fig. 5. Dated species-tree for the crested newts. Divergence times were determined with SNAPP, using a single *T. carnifex–T. macedonicus* inferred split date of 5.33 million years ago as a calibration point. Numbers at nodes reflect median divergence times in millions of years ago and bars the 95% credibility interval around the median.

Phylogenomics of the adaptive radiation of *Triturus* newts supports gradual ecological niche expansion towards an incrementally aquatic lifestyle

B. Wielstra, E. McCartney-Melstad, J.W. Arntzen, R.K. Butlin, H.B. Shaffer

SUPPLEMENTARY TEXT, FIGURES AND TABLES

SUPPLEMENTAL TEXT S1-S3

Text S1: Array Design

Transcriptome sequencing – Liver tissue samples in RNAlater from ten newts (one each of *Triturus anatolicus*, *T. carnifex*, *T. cristatus*, *T. dobrogicus*, *T. ivanbureschi*, *T. karelinii*, *T. macedonicus*, *T. marmoratus*, *T. pygmaeus*, and *Ommatotriton nesterovi*; Supplementary Table S1) were sent to ZF-Genomics (Leiden, The Netherlands) for RNA extraction and sequencing on a HiSeq 2500. Samples received an average of 43,810,415 clusters (SD=9,744,176) in 150bp paired-end configuration.

QC and Assembly – Paired-end sequencing reads were trimmed for adapter contamination and sequence quality using a 4-bp sliding window in Trimmomatic 0.32 (Bolger, et al. 2014), clipping the 3' ends of reads when the average sequence quality within the window dropped below 20. Leading bases with a quality score less than 5 and trailing bases with a quality score less than 15 were also removed, and reads shorter than 40bp after trimming were discarded.

A median of 38,575,204 read pairs were input into the Trinity assembler for each of the ten species (min=27,572,854, max=54,993,188, sd=8,916,227), and a median of 18.6% of these were

retained after *in silico* normalization (min=15.8%, max=22.8%, sd=2.3%). Each transcriptome was individually assembled using Trinity 2.2.0 with read coverage normalized to a maximum of 50 (Grabherr, et al. 2011). Individual Trinity assemblies were clustered at 90% identity using usearch v9.1.13 to reduce redundancy (Edgar 2010). Assemblies contained a median of 157,608 contigs after clustering at 90% similarity (min=80,803 for *T. karelinii*, and max=182,488 for *T. carnifex*).

These clustered assemblies were then used for pairwise comparison between *T. dobrogicus* and the other nine species using *blastn* v2.2.30 (Camacho, et al. 2009). The reciprocal best blast hits (RBBH) method was used to determine presumptive orthology between the assembled transcripts for each pairwise species comparison (Tatusov, et al. 1997; Bork, et al. 1998). *T. dobrogicus* transcripts that returned reciprocal best blast hits to all of the nine other species were retained and all other transcripts were discarded.

Transcriptome comparison – The remaining set of 10,333 *T. dobrogicus* transcripts was self-blasted to attempt to reduce redundancy, which may help reduce the inclusion of multiple isoforms of the same gene, chimeric transcripts assembled by Trinity, and transcripts with truly similar regions that may complicate downstream bioinformatics. As a conservative measure, both the subject and query transcript were discarded if any transcript showed significant similarity (blast e-value < 0.001) to a different transcript or to different regions of itself.

659 *Annotation* – The remaining set of 9,214 *T. dobrogicus* transcripts were annotated using a translated
660 blastx search to known *X. tropicalis* proteins with an e-value cutoff of 0.1 (Hellsten, et al. 2010).
661 Transcripts that did not have a positive blastx hit to the *Xenopus* protein database were discarded, and
662 only a single transcript annotating to a particular *Xenopus* protein was retained.

663

664 *Splice site prediction* – For the remaining set of 7,228 *T. dobrogicus* transcripts we attempted to infer
665 splice sites in the candidate targets to avoid designing baits that span such boundaries, as these baits
666 may perform poorly (Neves, et al. 2013) and because targeting a single exon for each transcript
667 simplifies downstream analyses. Splice sites were predicted by attempting to map each transcript to the
668 *Chrysemys picta* genome (Shaffer, et al. 2013) using exonerate's est2genome model (Slater and Birney
669 2005) with a DNA word length of 10. Approximately 93% of all transcripts (n=6,758) successfully
670 mapped to the *C. picta* genome, and for regions that mapped, the longest contiguous section of the
671 mapped transcript was harvested. If the longest contiguous segment was less than 200bp, the first high-
672 scoring segment pair (HSP) was extended towards the 5' end until reaching 200bp, followed by
673 extending the final HSP towards the 3' end until reaching 200bp if necessary. Of the 6,758 transcripts
674 that mapped to *C. picta*, 69 transcripts did not have an HSP longer than 200bp and could not be extended
675 to 200bp in the 5' or 3' direction and were dropped as prospective targets.

676 The 470 transcripts that did not align to the *C. picta* genome were sequentially aligned to the
677 genomes of *X. tropicalis* (Hellsten, et al. 2010), *Nanorana parkerii* (Sun, et al. 2015), and *Rana*
678 *catesbeiana* (Hammond, et al. 2017) to attempt to find splice sites, taking the first successful species
679 alignment from the list. Of these 470 transcripts, 125 mapped to *X. tropicalis*, 39 mapped to *N. parkerii*,
680 and 36 mapped to *R. catesbeiana*. Again the longest contiguous aligned segment of each transcript
681 was retained as a possible target, and transcripts with no aligned HSP of at least 200bp had their
682 alignments extended in the 5' then 3' directions to attain targets of at least 200bp. For the 270
683 transcripts that did not map to any genome, the first (leftmost) 300bp of the assembled transcript was
684 selected for a target region (except for the one transcript that was only 231bp long—for this target

685 the entire 231bp transcript was used). It is possible that this leftmost orientation may enrich these
686 targets for UTR sequence, assuming that the transcript was fully assembled by Trinity.

687 All exon targets were trimmed to a maximum of 450bp (from the 3' edge) and checked again
688 for complementarity using a self BLAST in blastn. The first qualifying target from each unique Trinity
689 cluster-gene identifier was retained, and any other targets that arose from the same Trinity gene
690 identifier were discarded (n=19). This target set contains sub-sequences from 7,139 different
691 transcripts for a total length of 2,272,851bp (mean of each sub-sequence=318bp, min=200bp,
692 max=400bp, median=300bp).

693 As we are interested in capturing these loci from all *Triturus* taxa, including both crested and
694 marbled newts, we decided to include probes designed from multiple species for the same target if
695 divergence between representative species in the two main clades was greater than 5% (Bi, et al.
696 2012). Since the bulk of the target sequences were designed from *T. dobrogicus*, which together with
697 *T. carnifex*, *T. cristatus* and *T. macedonicus* encompasses one of two main clades in the crested newts
698 (Wielstra and Arntzen 2011; Wielstra, Arntzen, et al. 2014), the three remaining species of crested
699 newts encompassing the other clade (*T. karelinii*, *T. anatolicus, and T. ivanbureschi*) were used to
700 determine if greater than 5% divergence existed between the two major clades for that target. First,
701 the *T. dobrogicus* targets were blasted against *T. karelinii*, enforcing a full-length HSP with respect to
702 the query sequence, yielding 2,850 hits; 30 of these were found to have a divergence greater than 5%
703 and were added to the 7,139 *T. dobrogicus* targets. Then the remaining 4,289 *T. dobrogicus* targets
704 were blasted to *T. anatolicus*, yielding 2,883 hits and an additional 35 targets. Finally the remaining
705 1,406 *T. dobrogicus* targets were blasted to *T. ivanbureschi*, yielding 631 hits and 10 more targets.
706 Subsequently the process was repeated for the marbled newts *T. pygmaeus* and *T. marmoratus*, which
707 constitute the sister lineage of the two crested newt clades, yielding an additional 222 and 27 targets
708 after positive hits for 5,544 of 7,139 targets and 440 of 1,595 residual targets, respectively. Overall, an
709 additional 324 orthologous targets that were more than 5% divergent between *T. dobrogicus* and

other *Triturus* species were added to attempt to generate a set of probes that would perform well across the genus.

A set of 7,463 target sequences (average length=317bp, min=175bp, max=474bp) was sent to Arbor Biosciences for probe tiling and synthesis. After removing any probes softmasked by RepeatMasker and the Amphibia database, 39,143 unique 120 bp RNA probes were synthesized at approximately 2.6X tiling density across 7,418 target sequences by Arbor Biosciences (Ann Arbor, MI) as a MyBaits-II kit.

Test for phylogenetic utility – The phylogenetic utility of the genomic transcript markers was validated by building a phylogeny from the transcript sequences with RAxML. Trinity-assembled transcriptomes were clustered at 90% identity using usearch v9.1.13 (Edgar 2010), and the sequence capture targets were aligned to these clusters using blastn v2.2.31 (Camacho, et al. 2009). The sequences corresponding to each target were extracted for each sample and aligned using mafft v7.313 (Katoh and Standley 2013) and all 7,139 sequence alignments (1 per target) were concatenated. RAxML v8.2.11(Stamatakis 2014) was used to generate a maximum likelihood phylogeny using 100 rapid bootstrap replicates and the GTRCAT model of sequence evolution. Results suggested sufficient phylogenetic resolution, but one unexpected finding was the placement of *T. carnifex* as the sister lineage to *T. dobrogicus* (Supplementary Fig. S1a). Yet, in our main experiment, *T. carnifex* was more closely related to *T. macedonicus* (see Results). The fact that the *T. carnifex* sample used for transcriptome sequencing originated from close to the documented hybrid zone with *T. dobrogicus* (Arntzen, et al. 2014; Wielstra, Sillero, et al. 2014) suggests that substantial interspecific gene flow might underlie this relationship. To further explore this scenario we obtained transcriptomes from two additional *T. carnifex* individuals, sampled away from the hybrid zone with *T. dobrogicus*, representing the distinct Balkan and Italian mtDNA clades (Canestrelli, et al. 2012; Wielstra, et al. 2013). We processed these two individuals as above and reran RAxML, replacing the *T. carnifex* sample from the hybrid zone, and found that *T. carnifex* was recovered as the sister lineage to *T. macedonicus* (Supplementary Fig. S1b). Assuming that the *T. carnifex*-*T. macedonicus* relationship is correct, this phylogenetic shift reflects both the

general risk of single-exemplar sampling (Spinks, et al. 2013) and the distorting influence that interspecific gene flow can have on phylogenetic inference (Leaché, et al. 2014). These findings support our decision to include multiple samples per species and to exclude samples from near known hybrid zones in our main experiment.

Text S2: Processing of Sequence Capture Data

Reference assembly – Sequence reads from the sample with the most reads (*T. carnifex* 292 with 3,937,346 read pairs) were used *de novo* to assemble target sequences for each target region. Trimmomatic v0.36 (Bolger, et al. 2014) was first used to remove adapter contamination and to trim leading bases with scores < 5, trailing bases with scores < 15, also employing a 4bp sliding window from 5' to 3', trimming the window and downstream sequence when the average quality of the window dropped < 20. Reads < 40bp were discarded. Trimmed reads were input into PEAR v0.9.10 (Zhang, et al. 2014) to merge overlapping paired end reads into longer single-end fragments with the following settings: p-value = 0.01, minimum assembly length = 50, statistical method = OES, using empirical frequencies = YES, quality score threshold = 0, minimum overlap = 10, and scaling method = scaled score.

Unmerged reads and merged read pairs were input into the assembly by reduced complexity (ARC) pipeline (Hunter, et al. 2015), which performs alternating tasks of mapping reads to target sequences, followed by per-target *de novo* assembly of mapped reads, replacing the original target sequences with the target assembly at each iteration. Six iterations were performed to generate a set of reference contigs assembled from reads relevant to each target region. A single assembled contig was then selected for each original target region by means of reciprocal best blast hit (RBBH) (Rivera, et al. 1998). These RBBHs were then blasted against one another to determine self-complementary regions, which can indicate chimeric assembly regions, and regions found to be similar to other target

762 regions were trimmed to the nearest terminus of the contig (McCartney-Melstad, et al. 2016). This set
763 of chimera-trimmed RBBHs was used as a target reference assembly for all downstream analyses.
764
765 *QC, SNP calling and genotyping* – Adapter contamination from library DNA inserts < 150bp was
766 removed from reads using skewer v0.2.2 (Jiang, et al. 2014). Reads were mapped to the reference
767 assembly using BWA-MEM v0.7.15-r1140 (Li 2013). Picard tools v2.9.2
768 (https://broadinstitute.github.io/picard/) was used to add read group information and mark PCR
769 duplicates, and GATK v3.8 was used to generate gVCFs for each sample using HaplotypeCaller.
770 GenotypeGVCFs was used for groups of samples (crested newts or crested + marbled newts, depending
771 on the analysis) to call SNPs/genotypes, removing SNPs flagged by the following hard filters: QD < 2,
772 MQ < 40, FS > 60, MQRankSum < -12.5, ReadPosRankSum < -8, QUAL < 30 (DePristo, et al. 2011;
773 Poplin, et al. 2017).

774 The *de novo* assembly followed by RBBH approach is susceptible to the inclusion of paralogous
775 loci as putatively single-copy targets. Because fixed differences between paralogues will appear as
776 consistently heterozygous SNPs, we next attempted to remove paralogous targets from our dataset
777 through the use of a Hardy Weinberg Equilibrium (HWE) filter for heterozygote excess. Heterozygote
778 excess p-values were calculated for every SNP using vcftools 0.1.15 (Danecek, et al. 2011), and any
779 target containing at least one SNP with a heterozygote excess p-value less than 0.05 was removed
780 from downstream analysis.
781
782 *Reference assembly and genotyping* – A total of 4,932,636 reads (including 2,579,319 merged read
783 pairs with an average length of 196bp) were used as input in the ARC assembly pipeline. After six
784 iterations of mapping and assembly, 6,970 targets finished with an average of 295 reads apiece
785 (median=167, sd=1,152), and 6,686 of the original targets had RBBHs to the assembly. After self-blast
786 and trimming to remove potentially chimeric assemblies, a reference assembly of 5,593,497bp was
787 generated for subsequent read mapping and SNP calling.

A median of 44.1% of trimmed reads aligned to the reference assembly (min=41.0%, max=50.5%), and an average of 22.6% of mapped reads were flagged as PCR duplicates, yielding a median unique reads on target of 34.2% (min=31.3%, max=39.4%). For the 23-sample dataset including the two marbled newt species, a total of 370,007 SNPs were recovered that passed hard filters. Of the 6,686 starting targets, 798 were found to contain at least 1 SNP with a HWE heterozygote excess p-value less than 0.05 and were removed. For the 21-sample dataset that did not contain the marbled newts, a total of 286,691 SNPs passed the hard filters and 814 targets were removed because they failed the HWE filter. Pairwise F84 divergences calculated with Phylip 3.697 (Felsenstein 1989) and based on the 23-sample dataset (including all *Triturus* species) are provided in Supplementary Table S2. The highest intraspecific divergence was observed between the Italian and Balkan clades comprising *T. carnifex*.

Text S3: Phylogenetic Analyses

Data concatenation with RAxML – RAxML version 8.2.11 (Stamatakis 2014) was used to infer phylogenies from concatenated alignments of SNPs. All biallelic SNPs in the 23-sample dataset that had genotype qualities of at least 20, that were present in at least 50% of the samples, and that fit RAxML's definition of variable (133,601 SNPs total across 5,866 different targets) were used for maximum likelihood phylogenetic analysis. 100 rapid bootstrap replicates and 20 maximum likelihood searches were conducted with the ASC_GTRGAMMA model with Lewis ascertainment correction for SNP analysis (Lewis 2001). The resulting phylogeny with bootstrap support values was plotted in R using phytools (Revell 2011).

The mean depth of passing genotype calls across all samples was 42.4X, and median per-site missingness was 4.3%, which corresponds to one sample out of 23 missing data for a site (mean=10.1%, sd=14.0%). All crested newt species (for which three individuals were included) were recovered as monophyletic, and all bootstrap values on the tree were 100 (Fig. 3). The longest branch was between

814 the marbled and crested newts and was used to root the tree. Within the crested newts, *T. ivanbureschi*
815 was the sister lineage to a clade consisting of *T. anatolicus* and *T. karelinii*. The remaining four species
816 were the sister-group to this assemblage, with *T. carnifex* most closely related to *T. macedonicus* and *T.*
817 *cristatus* most closely related to *T. dobrogicus*. Since the monophyly of all species was strongly
818 supported, species designations were fixed for subsequent species-tree inference.

819

820 *Gene-tree summary with ASTRAL* – ASTRAL v5.6.1 was used to estimate the crested newt phylogeny
821 and to explore gene-tree discordance, presumably derived primarily from incomplete lineage sorting
822 from a collection of gene-trees (Mirarab, et al. 2014; Sayyari and Mirarab 2016; Zhang, et al. 2017).
823 No marbled newts were included because estimating terminal branch lengths is not possible for species
824 with a single representative (note that the reciprocal monophyly of crested and marbled newts is well
825 established (Arntzen, et al. 2007; Espregueira Themudo, et al. 2009; Wielstra, Arntzen, et al. 2014) and
826 also strongly supported by our concatenated RAxML analysis). Separate polymorphic SNP alignments
827 were first generated for each target using SnpSift 4.3 (Ruden, et al. 2012) and PGDSpider 2.1.1.2
828 (Lischer and Excoffier 2012), omitting SNPs with > 50% missing data across the 21 crested newt
829 samples and removing targets that contained one or more samples with 100% missing data across the
830 target using trimal v1.4.1 (Capella-Gutiérrez, et al. 2009). RAxML v8.2.11 (Stamatakis 2014) was used
831 to infer a maximum likelihood gene-tree for each target with the ASC_GTRGAMMA model and Lewis
832 ascertainment bias correction (Lewis 2001).

833 After setting genotypes with quality scores less than 20 to missing data and filtering out sites
834 with > 50% missing data, a total of 143,571 SNPs remained across 5,861 targets to build gene-trees.
835 After removing targets that contained samples with 100% missing data and removing sites that RAxML
836 determined to be monomorphic, maximum likelihood gene-trees were built for 5,610 targets. These
837 gene-trees were used as input into ASTRAL, constraining the seven crested newt species to be
838 monophyletic (as supported by our concatenated RAxML analysis) and outputting local posterior
839 probabilities and inferring terminal branch lengths. Midpoint rooting was used to determine the root.
840 ASTRAL yielded a final normalized quartet score of 0.63. The same topology as in the concatenated

RAxML analysis was recovered, with local posterior probabilities of 1 for all nodes (Fig. 4a). Branch lengths in ASTRAL are measured in coalescent units and indicate the degree of discordance among gene-trees (within taxa for terminal branches and among taxa for internal branches). The longest terminal branch was recovered for *T. macedonicus*, and the shortest belonged to *T. anatolicus*. The shortest internal branches were those separating the sister lineages *T. carnifex* + *T. macedonicus* from *T. cristatus* + *T. dobrogicus*.

Species-tree estimation with SNAPP – The coalescent species-tree inference method SNAPP v1.3.0 was used to infer the crested newt species-tree from biallelic SNPs (Bryant, et al. 2012). Marbled newts were not included because they introduce a long internal branch that can render parameter estimation inaccurate and splits between them and crested newts is not a primary goal of our paper. Polymorphic biallelic SNPs with genotype phred scores ≥ 20 across all 21 crested newts were first collected. Then, a single SNP from each of the 5,581 remaining loci was randomly selected to reduce the impacts of physical genetic linkage. These SNPs were used as input into SNAPP within the BEAST v2.4.8 environment (Bouckaert, et al. 2014) with the following parameters: species assignment=7 respective species, mutation rate U=1.0, mutation rate V=1.0, coalescence rate=10.0 (and sampled), use log likelihood correction=True, lambda prior=Gamma (initial=10[0.0,inf]) with alpha=2.0 and beta=200.0, snapprior.alpha=1.0, snapprior.beta=250.0, snapprior.kappa=1.0, snapprior.lambda=10.0 (and sampled), snapprior.rateprior=gamma, chain length=10,000,000, store every=1000 (and logging every 1000), and pre burnin=0. A 10% burnin was used and convergence and mixing were assessed with Tracer v1.7.1 (Rambaut, et al. 2018). ESS values for all parameters were > 400. A maximum clade credibility tree was constructed with common ancestor heights using TreeAnnotator v2.4.8 (Bouckaert, et al. 2014). Note that BEAST infers the root as part of the analysis. The same topology as in the RAxML and ASTRAL analyses was recovered (Fig. 4b). All posterior probabilities were 1, except for the node subtending *T. carnifex* + *T. macedonicus*, which was 0.99.

867 *Molecular dating with SNAPP* – A time-calibrated phylogeny was estimated with SNAPP using the same
868 input SNP file as above. For calibration we interpreted the origin of the Adriatic Sea at the end of the
869 Messinian Salinity Crisis at 5.33 million years ago (Krijgsman, et al. 1999) as the vicariance event
870 causing the *T. carnifex* versus *T. macedonicus* split (Arntzen, et al. 2007; Wielstra and Arntzen 2011)
871 and set the age of their most recent common ancestor to a uniform distribution between 5.32 and
872 5.34 million years ago (Stange, et al. 2018). Input XML files for divergence time estimation were
873 prepared using snapp_prep.rb (https://github.com/mmatschiner/snapp_prep). We recognize that
874 this is only a rough approximation given a single, biogeographically-informed date calibration point,
875 and use it primarily to estimate the closeness in time of the crested newt radiation. The output tree
876 from the original, undated SNAPP analysis was used as a starting tree, scaling the entire tree so that
877 the starting age of the calibration node was 5.33 million years ago. The topology was fixed to that
878 recovered by the original SNAPP analysis, and dates of remaining nodes were estimated using
879 1,000,000 MCMC steps, sampling every 500 steps and removing a 10% burn-in. ESS values for
880 parameters were confirmed > 400 with Tracer. A maximum clade credibility tree with median node
881 heights was generated with TreeAnnotator (Fig. 5).
882
883 **Text S4: Comparison with full mtDNA-based phylogeny**
884
885 MtDNA has proven misleading at both recent (Rodríguez, et al. 2017) and deeper (Veith, et al. 2018)
886 nodes in the Salamandridae phylogeny and our genome-enabled phylogeny shows a highly supported
887 deviation with a previous full mtDNA (i.e. single marker) phylogeny as well (Wielstra and Arntzen 2011).
888 The deviation concerns the relationship among the three species constituting the '*T. karelinii*-group';
889 we here recover *T. anatolicus* as the sister lineage to *T. karelinii*, rather than to *T. ivanbureschi* as
890 suggested by mtDNA (Supplementary Fig. S2). While such gene-tree discordance could reflect
891 incomplete lineage sorting of mtDNA (Platt, et al. 2018), we consider ancient mtDNA introgression

892 more likely, as *T. ivanbureschi* and *T. anatolicus* show geographically extensive introgressive
893 hybridization today (Wielstra, et al. 2017). A scenario of ancient introgression is in line with the high
894 degree of gene-tree/species-tree discordance in the nuclear genome in *T. anatolicus*, as suggested by
895 the short branch in the ASTRAL tree (Fig. 4a). However, as all members of the '*T. karelinii*-group'
896 possess an identical number of trunk vertebrae, the mtDNA-nuDNA mismatch does not influence our
897 interpretation of character evolution (Supplementary Fig. S3). The calibrated nuclear DNA-based (Fig.
898 5) and mtDNA-based phylogenies agree that cladogenesis among crested newts occurred over a
899 relatively brief time window. However, mtDNA-based dates are older (cf. Table 2 in Wielstra and
900 Arntzen 2011). This could simply reflect the differences in the dating method and the (slight)
901 differences in the calibration scheme applied, but it is well-known that divergence times derived from
902 individual gene-trees, and particularly from mtDNA, can be overestimates of lineage divergence
903 (McCormack, et al. 2011).
904
905 **Text S5: Inference of changes in the number of trunk vertebrae**
906 The number of trunk vertebrae (NTV) in crested newts is characterized by a punctuated continuous
907 character state distribution, with modal values for NTV in the range of 13-16 (for convenience an NTV
908 count of 16 was used for *T. dobrogicus*, but note that NTV = 17 also occurs at roughly equal frequency
909 in this species, which does not influence our interpretation). We consider NTV = 12, as observed in the
910 sister lineage the marbled newts (the *T. marmoratus*-group), as well as the most closely related genus
911 *Lissotriton*, to be the ancestral state (Arntzen, et al. 2015; Veith, et al. 2018). We applied the parsimony
912 criterion to infer changes in NTV along all possible crested newt topologies (Supplementary Fig. S3).
913 The program PAUP* (Swofford 1998) was used to allocate character state gains and losses over the
914 tree, under ACCTRAN as well as DELTRAN optimization.
915
916 **References**

Arntzen JW, Beukema W, Galis F, Ivanović A. 2015. Vertebral number is highly evolvable in salamanders and newts (family Salamandridae) and variably associated with climatic parameters. Contributions to Zoology 84:85-113.

Arntzen JW, Espregueira Themudo G, Wielstra B. 2007. The phylogeny of crested newts (*Triturus cristatus* superspecies): nuclear and mitochondrial genetic characters suggest a hard polytomy, in line with the paleogeography of the centre of origin. Contributions to Zoology 76:261-278.

Arntzen JW, Wielstra B, Wallis GP. 2014. The modality of nine *Triturus* newt hybrid zones, assessed with nuclear, mitochondrial and morphological data. Biological Journal of the Linnean Society 113:604–622.

Bi K, Vanderpool D, Singhal S, Linderoth T, Moritz C, Good JM. (Bi2012 co-authors). 2012. Transcriptome-based exon capture enables highly cost-effective comparative genomic data collection at moderate evolutionary scales. BMC Genomics 13:403.

Bolger AM, Lohse M, Usadel B. 2014. Trimmomatic: a flexible trimmer for Illumina sequence data. Bioinformatics 30:2114-2120.

Bork P, Dandekar T, Diaz-Lazcoz Y, Eisenhaber F, Huynen M, Yuan Y. 1998. Predicting function: from genes to genomes and back. Journal of Molecular Biology 283:707-725.

Bouckaert R, Heled J, Kühnert D, Vaughan T, Wu C-H, Xie D, Suchard MA, Rambaut A, Drummond AJ. 2014. BEAST 2: a software platform for Bayesian evolutionary analysis. PLoS Computational Biology 10:e1003537.

Bryant D, Bouckaert R, Felsenstein J, Rosenberg NA, RoyChoudhury A. 2012. Inferring species trees directly from biallelic genetic markers: bypassing gene trees in a full coalescent analysis. Molecular Biology and Evolution 29:1917-1932.

Camacho C, Coulouris G, Avagyan V, Ma N, Papadopoulos J, Bealer K, Madden TL. 2009. BLAST+: architecture and applications. BMC Bioinformatics 10:421-421.

Canestrelli D, Salvi D, Maura M, Bologna MA, Nascetti G. 2012. One Species, three Pleistocene evolutionary histories: phylogeography of the Italian crested newt, *Triturus carnifex*. PLoS ONE 7:e41754.

Capella-Gutiérrez S, Silla-Martínez JM, Gabaldón T. 2009. trimAl: a tool for automated alignment trimming in large-scale phylogenetic analyses. Bioinformatics 25:1972-1973.

Danecek P, Auton A, Abecasis G, Albers CA, Banks E, DePristo MA, Handsaker RE, Lunter G, Marth GT, Sherry ST, et al. 2011. The variant call format and VCFtools. Bioinformatics 27:2156-2158.

DePristo MA, Banks E, Poplin R, Garimella KV, Maguire JR, Hartl C, Philippakis AA, del Angel G, Rivas MA, Hanna M, et al. 2011. A framework for variation discovery and genotyping using next-generation DNA sequencing data. Nature Genetics 43:491-498.

Edgar RC. 2010. Search and clustering orders of magnitude faster than BLAST. Bioinformatics 26:2460-2461.

955 Espregueira Themudo G, Wielstra B, Arntzen JW. 2009. Multiple nuclear and mitochondrial
956 genes resolve the branching order of a rapid radiation of crested newts (*Triturus*,
957 Salamandridae). Molecular Phylogenetics and Evolution 52:321-328.

958 Felsenstein J. 1989. PHYLIP - Phylogeny Inference Package (Version 3.2). Cladistics 5:164-
959 166.

960 Grabherr MG, Haas BJ, Yassour M, Levin JZ, Thompson DA, Amit I, Adiconis X, Fan L,
961 Raychowdhury R, Zeng Q, et al. 2011. Full-length transcriptome assembly from RNA-Seq data
962 without a reference genome. Nature Biotechnology 29:644-652.

963 Hammond SA, Warren RL, Vandervalk BP, Kucuk E, Khan H, Gibb EA, Pandoh P, Kirk H,
964 Zhao Y, Jones M, et al. 2017. The North American bullfrog draft genome provides insight into
965 hormonal regulation of long noncoding RNA. Nature Communications 8:1433.

966 Hellsten U, Harland RM, Gilchrist MJ, Hendrix D, Jurka J, Kapitonov V, Ovcharenko I,
967 Putnam NH, Shu S, Taher L, et al. 2010. The genome of the western clawed frog *Xenopus*
968 *tropicalis*. Science 328:633.

969 Hunter SS, Lyon RT, Sarver BAJ, Hardwick K, Forney LJ, Settles ML. 2015. Assembly by
970 Reduced Complexity (ARC): a hybrid approach for targeted assembly of homologous
971 sequences. bioRxiv.

972 Jiang H, Lei R, Ding S-W, Zhu S. 2014. Skewer: a fast and accurate adapter trimmer for next-
973 generation sequencing paired-end reads. BMC Bioinformatics 15:182.

974 Katoh K, Standley DM. 2013. MAFFT Multiple Sequence Alignment Software Version 7:
975 Improvements in Performance and Usability. Molecular Biology and Evolution 30:772-780.

976 Krijgsman W, Hilgen FJ, Raffi I, Sierro FJ, Wilson DS. 1999. Chronology, causes and
977 progression of the Messinian salinity crisis. Nature 400:652-655.

978 Leaché AD, Harris RB, Rannala B, Yang Z. 2014. The influence of gene flow on species tree
979 estimation: a simulation study. Systematic Biology 63:17-30.

980 Lewis PO. 2001. A likelihood approach to estimating phylogeny from discrete morphological
981 character data. Systematic Biology 50:913-925.

982 Li H. 2013. Aligning sequence reads, clone sequences and assembly contigs with BWA-MEM.
983 arXiv preprint arXiv:1303.3997.

984 Lischer HEL, Excoffier L. 2012. PGDSpider: an automated data conversion tool for connecting
985 population genetics and genomics programs. Bioinformatics 28:298-299.

986 McCartney-Melstad E, Mount GG, Bradley Shaffer H. 2016. Exon capture optimization in
987 amphibians with large genomes. Molecular Ecology Resources 16:1084-1094.

988 McCormack JE, Heled J, Delaney KS, Peterson AT, Knowles LL. 2011. Calibrating divergence
989 times on species trees versus gene trees: implications for speciation history of *Aphelocoma* jays.
990 Evolution 65:184-202.

991 Mirarab S, Reaz R, Bayzid MS, Zimmermann T, Swenson MS, Warnow T. 2014. ASTRAL:
992 genome-scale coalescent-based species tree estimation. Bioinformatics 30:i541-i548.

993 Neves LG, Davis JM, Barbazuk WB, Kirst M. 2013. Whole-exome targeted sequencing of the
994 uncharacterized pine genome. The Plant Journal 75:146-156.

995 Platt IIRN, Faircloth BC, Sullivan KAM, Kieran TJ, Glenn TC, Vandewege MW, Lee JTE,
996 Baker RJ, Stevens RD, Ray DA. 2018. Conflicting evolutionary histories of the mitochondrial
997 and nuclear genomes in New World *Myotis* bats. Systematic Biology 67:236-249.

998 Poplin R, Ruano-Rubio V, DePristo MA, Fennell TJ, Carneiro MO, Van der Auwera GA, Kling
999 DE, Gauthier LD, Levy-Moonshine A, Roazen D, et al. 2017. Scaling accurate genetic variant
1000 discovery to tens of thousands of samples. bioRxiv.

1001 Rambaut A, Drummond AJ, Xie D, Baele G, Suchard MA. 2018. Posterior summarization in
1002 Bayesian phylogenetics using Tracer 1.7. Systematic Biology:syy032-syy032.

1003 Revell LJ. 2011. phytools: an R package for phylogenetic comparative biology (and other
1004 things). Methods in Ecology and Evolution 3:217-223.

1005 Rivera MC, Jain R, Moore JE, Lake JA. 1998. Genomic evidence for two functionally distinct
1006 gene classes. Proceedings of the National Academy of Sciences of the United States of America
1007 95:6239-6244.

1008 Rodríguez A, Burgon JD, Lyra M, Irisarri I, Baurain D, Blaustein L, Göçmen B, Künzel S,
1009 Mable BK, Nolte AW, et al. 2017. Inferring the shallow phylogeny of true salamanders
1010 (*Salamandra*) by multiple phylogenomic approaches. Molecular Phylogenetics and Evolution
1011 115:16-26.

1012 Ruden D, Cingolani P, Patel V, Coon M, Nguyen T, Land S, Lu X. 2012. Using *Drosophila*
1013 *melanogaster* as a model for genotoxic chemical mutational studies with a new program,
1014 SnpSift. Frontiers in Genetics 3.

1015 Sayyari E, Mirarab S. 2016. Fast coalescent-based computation of local branch support from
1016 quartet frequencies. Molecular Biology and Evolution 33:1654-1668.

1017 Shaffer HB, Minx P, Warren DE, Shedlock AM, Thomson RC, Valenzuela N, Abramyan J,
1018 Amemiya CT, Badenhorst D, Biggar KK, et al. (Bradley Shaffer2013 co-authors). 2013. The
1019 western painted turtle genome, a model for the evolution of extreme physiological adaptations
1020 in a slowly evolving lineage. Genome Biology 14:R28.

1021 Slater GSC, Birney E. 2005. Automated generation of heuristics for biological sequence
1022 comparison. BMC Bioinformatics 6:31.

1023 Spinks PQ, Thomson RC, Pauly GB, Newman CE, Mount G, Shaffer HB. 2013. Misleading
1024 phylogenetic inferences based on single-exemplar sampling in the turtle genus *Pseudemys*.
1025 Molecular Phylogenetics and Evolution 68:269-281.

1026 Stamatakis A. 2014. RAxML version 8: a tool for phylogenetic analysis and post-analysis of
1027 large phylogenies. Bioinformatics 30:1312-1313.

Stange M, Sánchez-Villagra MR, Salzburger W, Matschiner M. 2018. Bayesian divergence-time estimation with genome-wide Single-Nucleotide Polymorphism data of sea catfishes (Ariidae) supports Miocene closure of the Panamanian isthmus. Systematic Biology 67:681-699.

Sun Y-B, Xiong Z-J, Xiang X-Y, Liu S-P, Zhou W-W, Tu X-L, Zhong L, Wang L, Wu D-D, Zhang B-L, et al. 2015. Whole-genome sequence of the Tibetan frog *Nanorana parkeri* and the comparative evolution of tetrapod genomes. Proceedings of the National Academy of Sciences of the United States of America 112:E1257.

Swofford DL. 1998. PAUP 4.0b: Phylogenetic Analysis Using Parsimony. Sunderland: Sinauer Associates.

Tatusov RL, Koonin EV, Lipman DJ. 1997. A genomic perspective on protein families. Science 278:631.

Veith M, Bogaerts S, Pasmans F, Kieren S. 2018. The changing views on the evolutionary relationships of extant Salamandridae (Amphibia: Urodela). PLoS ONE 13:e0198237.

Wielstra B, Arntzen JW. 2011. Unraveling the rapid radiation of crested newts (*Triturus cristatus* superspecies) using complete mitogenomic sequences. BMC Evolutionary Biology 11:162.

Wielstra B, Arntzen JW, van der Gaag K, Pabijan M, Babik W. 2014. Data concatenation, Bayesian concordance and coalescent-based analyses of the species tree for the rapid radiation of *Triturus* newts. PLoS ONE 9:e111011.

Wielstra B, Burke T, Butlin RK, Avcı A, Üzüm N, Bozkurt E, Olgun K, Arntzen JW. 2017. A genomic footprint of hybrid zone movement in crested newts. Evolution Letters 1:93-101.

Wielstra B, Crnobrnja-Isailović J, Litvinchuk SN, Reijnen BT, Skidmore AK, Sotiropoulis K, Toxopeus AG, Tzankov N, Vukov T, Arntzen JW. 2013. Tracing glacial refugia of *Triturus* newts based on mitochondrial DNA phylogeography and species distribution modeling. Frontiers in Zoology 10:13.

Wielstra B, Sillero N, Vörös J, Arntzen JW. 2014. The distribution of the crested and marbled newt species (Amphibia: Salamandridae: *Triturus*) – an addition to the New Atlas of Amphibians and Reptiles of Europe. Amphibia-Reptilia 35:376-381.

Zhang C, Sayyari E, Mirarab S editors. Comparative Genomics. 2017 2017//: Cham.

Zhang J, Kobert K, Flouri T, Stamatakis A. 2014. PEAR: a fast and accurate Illumina Paired-End reAd mergeR. Bioinformatics 30:614-620.

SUPPLEMENTARY FIGURES S1-S3

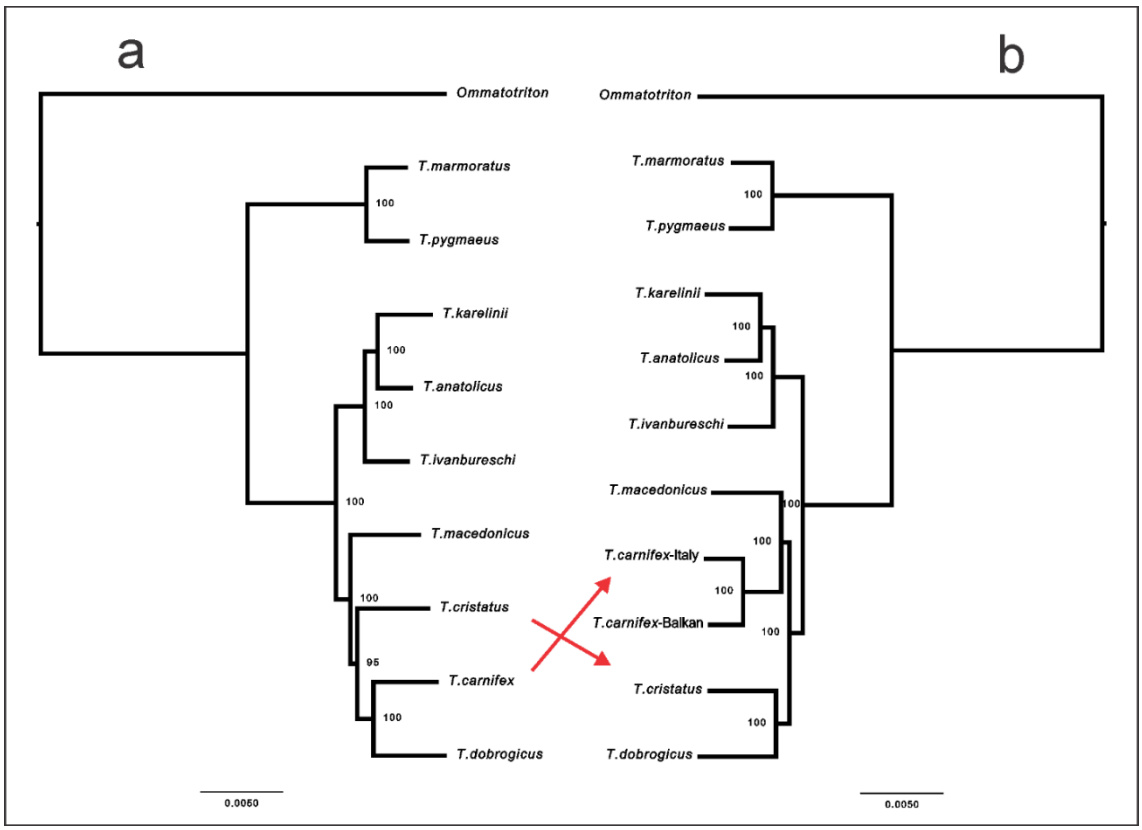

Fig. S1. *Triturus* newt phylogenies based on based on data concatenation of transcriptome data with RAxML. In a) a *T. carnifex* individual is included that is suspected to be admixed with *T. dobrogicus* and in b) this is replaced by two other *T. carnifex* individuals assumed to not be affected by genetic admixture, one from the Balkans and one from Italy, away from the contact zone with *T. dobrogicus*. Note the differences in sister species relationships (reflected by red arrows), with the phylogeny in b) being in full agreement with the one based on target capture data (Fig. 3; Fig. 4).

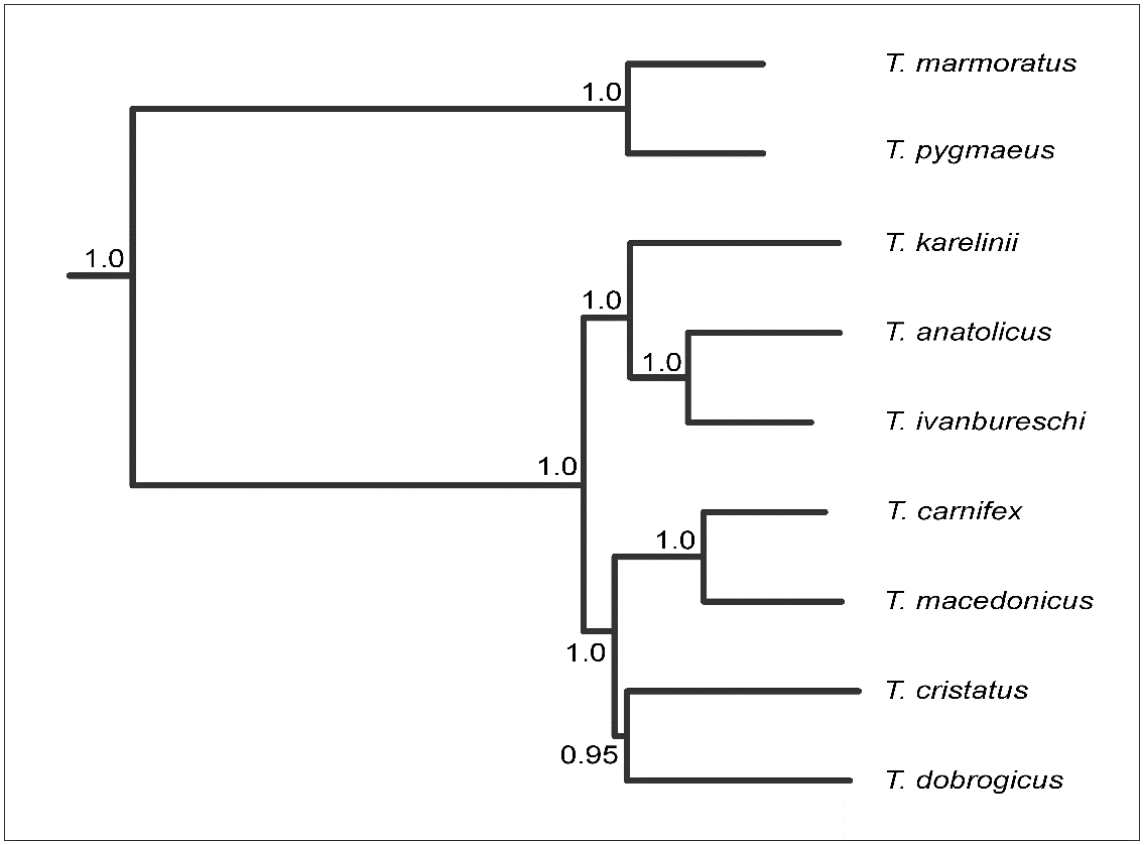

Fig. S2. Full mtDNA phylogeny for *Triturus*. The genome-enabled *Triturus* phylogeny (Fig. 3; Fig. 4) deviates from the phylogeny based on full mtDNA (taken from (Wielstra and Arntzen 2011)) for the species relationships in the *T. karelinii*-group of crested newts (with *T. anatolicus* being sister to *T. karelinii* rather than *T. ivanbureschi*). Numbers at nodes indicate posterior probabilities. Note the relatively low support for the sister relationship between *T. cristatus* and *T. dobrogicus*.

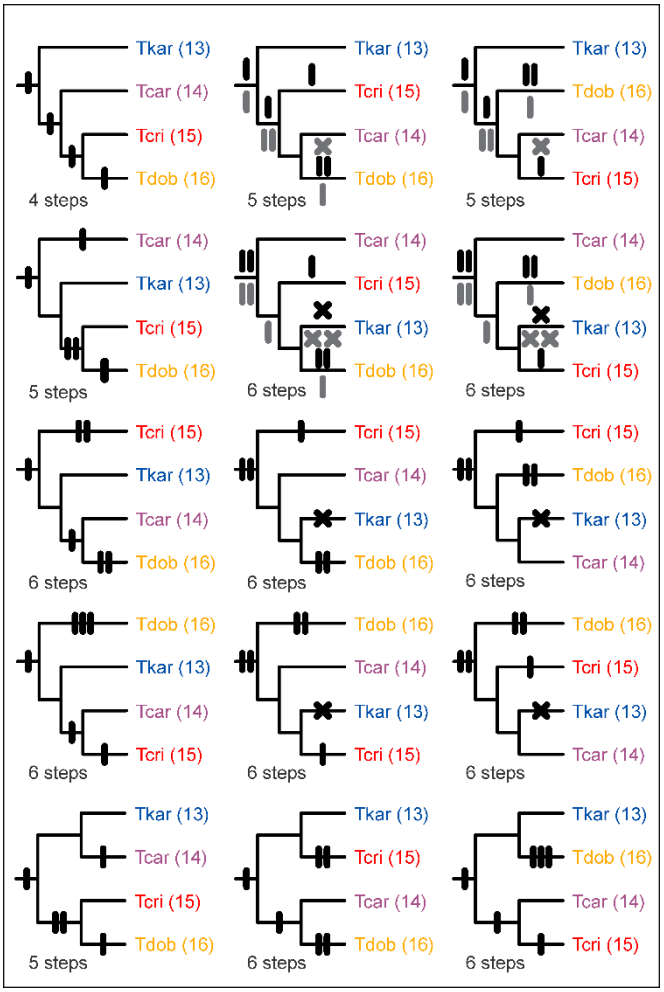

Fig. S3. All 15 topologies possible for a fully bifurcating phylogeny of the four crested newt body builds. Abbreviations: Tkar = *T. karelinii*-group; Tcar = *T. carnifex*-group; Tcri = *T. cristatus*; Tdob = *T. dobrogicus*. The number of trunk vertebrae (NTV) for each body build is provided in parentheses. A bar represents an NTV addition and a cross a deletion. NTV changes were inferred under the parsimony criterion, considering NTV = 12 as the ancestral character state for *Triturus* (see Supplementary Text S5). Results under ACCTRAN and DELTRAN optimization were identical for 11 topologies; for the four ones that deviated, character state changes under DELTRAN optimization are in black and above and under ACCTRAN optimization in grey and below branches. The top left topology corresponds to the *Triturus* species tree (Fig. 3; Fig. 4).

SUPPLEMENTARY TABLES S1-S2

Table S1. Sampling details. Individuals are identified with a code that refers to complete specimens (ID starting with ZMA) or tail tips (remaining samples). All material is stored at Naturalis Biodiversity Center, Leiden, The Netherlands.

Target capture

ID	Species	Locality	Latitud	Longitud
5017	*Triturus marmoratus*	France: Jublains	48.252	-0.473
5016	*Triturus pygmaeus*	Portugal: Serra de Monchique	37.335	-8.506
4729	*Triturus ivanbureschi*	Bulgaria: Ostar Kamak	41.878	25.853
1814	*Triturus ivanbureschi*	Turkey: Karakadılar	40.010	26.940
1788	*Triturus ivanbureschi*	Turkey: Bozdağ	38.367	28.103
1847	*Triturus anatolicus*	Turkey: Abanta Gölu	40.612	31.288
1889	*Triturus anatolicus*	Turkey: Gölköy	40.083	33.347
1985	*Triturus anatolicus*	Turkey: Çakırlı	40.446	37.483
2105	*Triturus karelinii*	Ukraine: Nikita	44.538	34.243
6719	*Triturus karelinii*	Azerbaijan: Altiagac	40.854	48.935
RMNH RenA 46931-2390	*Triturus karelinii*	Iran: Qu'Am Shahr	36.436	52.803
ZMA9108-405	*Triturus carnifex*	Italy: Fuscaldo	39.417	16.033
ZMA9145-292	*Triturus carnifex*	Italy: Pisa	43.717	10.400
ZMA9132-312	*Triturus carnifex*	Slovenia: Kramplje	45.733	14.500
3247	*Triturus macedonicus*	Montenegro: Bjeloši	42.374	18.907
3275	*Triturus macedonicus*	Albania: Bejar	40.429	19.850
3775	*Triturus macedonicus*	Greece: Kerameia	39.562	22.081
4485	*Triturus cristatus*	Bulgaria: Montana	43.416	23.222
3686	*Triturus cristatus*	Romania: Budeni	45.768	26.839
ZMA9167-355	*Triturus cristatus*	Romania: Virfuri	46.283	22.467
ZMA9083-512	*Triturus dobrogicus*	Hungary: Alap	46.800	18.683
ZMA9172-720	*Triturus dobrogicus*	Croatia: Zupanja	45.083	18.700
2377	*Triturus dobrogicus*	Romania: Măcin	45.251	28.121

Transcriptomes

ID	Species	Locality	Latitud	Longitud
6720	*Triturus marmoratus*	Portugal: Valongo	41.168	-8.500
6721	*Triturus pygmaeus*	Portugal: Serra de Monchique	37.335	-8.506
6722	*Triturus karelinii*	Azerbaijan: Katex	41.646	46.543
6723	*Triturus anatolicus*	Turkey: Hacılar	41.495	32.088
6724	*Triturus ivanbureschi*	Turkey: Keşan	40.924	26.635
6725	*Triturus carnifex*	Croatia: Prkovac	45.569	16.094
6726	*Triturus carnifex*	Croatia: Radetići	45.146	13.842
6727	*Triturus carnifex*	Italy: Viterbo	42.703	13.325
6728	*Triturus macedonicus*	Montenegro: Ceklin	42.367	18.982
6729	*Triturus cristatus*	France: Belgeard	48.259	-0.574
6730	*Triturus dobrogicus*	Serbia: Sremski Karlovski	45.175	19.991
6731	*Ommatotriton nesterovi*	Turkey: Hürriyet	40.276	28.650

Table S2. Inter- and intraspecific divergence in *Triturus* newts. Shown are pairwise F84 divergences calculated with Phylip. Intraspecific distances are in italics. IDs correspond to Supplementary Table S1.

		5017	**5016**	**4729**	**1814**	**1788**	**1847**	**1889**	**1985**	**2105**	**6719**	**2390**	**405**	**292**	**312**	**3247**	**3275**	**3775**	**4485**	**3686**	**355**	**512**	**720**	**2377**
T. marmoratus	**5017**	-																						
T. pygmaeus	**5016**	0.10	-																					
T. ivanbureschi	**4729**	0.72	0.70	-																				
	1814	0.72	0.70	*0.02*	-																			
	1788	0.72	0.71	*0.03*	*0.02*	-																		
T. anatolicus	**1847**	0.68	0.66	0.08	0.08	0.09	-																	
	1889	0.72	0.70	0.11	0.11	0.12	*0.02*	-																
	1985	0.72	0.70	0.11	0.11	0.12	*0.03*	*0.03*	-															
T. karelinii	**2105**	0.71	0.69	0.14	0.14	0.14	0.09	0.11	0.11	-														
	6719	0.74	0.72	0.14	0.14	0.15	0.10	0.12	0.11	*0.01*	-													
	2390	0.73	0.71	0.14	0.14	0.15	0.10	0.12	0.11	*0.01*	*0.02*	-												
T. carnifex	**405**	0.74	0.72	0.25	0.25	0.26	0.23	0.26	0.25	0.27	0.27	0.27	-											
	292	0.75	0.73	0.25	0.25	0.26	0.23	0.26	0.25	0.26	0.27	0.27	*0.03*	-										
	312	0.71	0.69	0.23	0.23	0.24	0.21	0.24	0.23	0.25	0.25	0.25	*0.08*	*0.07*	-									
T. macedonicus	**3247**	0.74	0.72	0.24	0.24	0.25	0.22	0.25	0.25	0.25	0.26	0.26	0.22	0.21	0.19	-								
	3275	0.72	0.70	0.23	0.23	0.23	0.20	0.23	0.23	0.24	0.24	0.24	0.20	0.20	0.18	*0.04*	-							
	3775	0.75	0.73	0.24	0.24	0.25	0.22	0.25	0.25	0.26	0.26	0.26	0.22	0.22	0.20	*0.06*	*0.04*	-						
T. cristatus	**4485**	0.71	0.69	0.21	0.21	0.22	0.19	0.22	0.21	0.23	0.23	0.23	0.21	0.21	0.19	0.20	0.18	0.20	-					
	3686	0.72	0.70	0.22	0.22	0.22	0.20	0.22	0.22	0.23	0.24	0.24	0.21	0.21	0.19	0.20	0.18	0.20	*0.05*	-				
	355	0.69	0.67	0.21	0.21	0.21	0.19	0.21	0.21	0.22	0.23	0.23	0.21	0.21	0.19	0.19	0.17	0.19	*0.04*	*0.05*	-			
T. dobrogicus	**512**	0.71	0.69	0.23	0.23	0.24	0.21	0.24	0.23	0.25	0.25	0.25	0.21	0.20	0.18	0.21	0.19	0.21	0.17	0.17	0.17	-		
	720	0.69	0.67	0.21	0.21	0.22	0.20	0.22	0.22	0.23	0.23	0.23	0.19	0.18	0.17	0.19	0.17	0.19	0.16	0.16	0.16	*0.03*	-	
	2377	0.70	0.68	0.22	0.22	0.22	0.20	0.22	0.22	0.23	0.24	0.24	0.19	0.19	0.17	0.19	0.18	0.19	0.15	0.16	0.15	*0.02*	*0.03*	-